

# Demystifying Spatial Confounding

Emiko Dupont<sup>1</sup>(eahd20@bath.ac.uk), Isa Marques<sup>2</sup>, and Thomas Kneib<sup>3</sup>,

<sup>1</sup>Department of Mathematical Sciences, University of Bath,  
Claverton Down, Bath BA2 7AY, U.K.

<sup>2</sup> Department of Statistics, The Ohio State University,  
Cockins Hall, 1958 Neil Ave, Columbus 43210, U.S.A.

<sup>3</sup>Chair of Statistics and Campus Institute Data Science, University of Göttingen,  
Humboldtallee 3, 37073 Göttingen, Germany

## Abstract

Spatial confounding is a fundamental issue in spatial regression models which arises because spatial random effects, included to approximate unmeasured spatial variation, are typically not independent of covariates in the model. This can lead to significant bias in covariate effect estimates. The problem is complex and has been the topic of extensive research with sometimes puzzling and seemingly contradictory results. Here, we develop a broad theoretical framework that brings mathematical clarity to the mechanisms of spatial confounding, deriving an explicit analytical expression for the resulting bias. We see that the problem is directly linked to spatial smoothing and identify exactly how the size and occurrence of bias relate to the features of the spatial model as well as the underlying confounding scenario. Using our results, we can explain subtle and counter-intuitive behaviours. Finally, we propose a general approach for dealing with spatial confounding bias in practice, applicable for any spatial model specification. When a covariate has non-spatial information, we show that a general form of the so-called spatial+ method can be used to eliminate bias. When no such information is present, the situation is more challenging but, under the assumption of unconfounded high frequencies, we develop a procedure in which multiple capped versions of spatial+ are applied to assess the bias in this case. We illustrate our approach with an application to air temperature in Germany.

**Keywords:** Confounding bias; spatial regression; spatial random effects; smoothing; spatial+.

## 1 Introduction

In spatial statistics, regression models usually take the form

$$y(s) = \beta x(s) + \gamma(s) + \epsilon(s) \quad (1)$$

where  $y(s)$  denotes the response variable of interest,  $x(s)$  a covariate with regression coefficient  $\beta$ ,  $\gamma(s)$  a spatially correlated random effect and  $\epsilon(s)$  independent and identically distributed error terms, all evaluated at locations  $s$  within some spatial domain. The spatial effect  $\gamma(s)$  is included to approximate unmeasured spatial variation in the response which typically arises due to unobserved spatial variables. Specific instances of the model are obtained by specifying the type of spatial information (e.g. discrete regional vs. continuous coordinate-based) and the representation of the spatial effect  $\gamma(s)$  (e.g. Gaussian random fields, Markov random fields, thin plate splines, etc.).

Although not always explicitly stated, the regression (1) assumes that the covariate  $x(s)$  is given and fixed. This implies independence between the covariate and the spatial effect, which is unlikely to hold for observational data where covariates are realisations of potentially spatially dependent random variables. If indeed this assumption is violated, it leads to a phenomenon known as spatial confounding, where the estimate of the covariate effect  $\beta$  becomes biased even when the model is correctly specified. Thus, understanding spatial confounding is fundamental to reliable estimation of covariate effects in spatial statistics, and the problem has received considerable attention in the literature since the seminal work of Clayton et al. (1993) and, later, Hodges and Reich (2010). Recently, there has been a surge in interest, not least because the established understanding and methods most commonly used for dealing with the problem have been shown to be problematic.

Broadly, research into spatial confounding can be structured along the following lines: (i) Investigations and suggestions for potential solutions under specific instances of the model (1) such as a choice of discrete or continuous spatial dependence and/or a particular representation of the spatial effect (Dupont et al., 2022; Guan et al., 2023; Marques et al., 2022; Urdangarin Iztueta et al., 2022). (ii) Identifying factors that influence the size or occurrence of bias, in particular, the importance of the spatial scales of both measured and unmeasured variables (Paciorek, 2010; Page et al., 2017; Keller and Szpiro, 2020; Nobre et al., 2021; Bobb et al., 2022). (iii) Research based on a (sometimes implicit) preference for the estimate of  $\beta$  in a non-spatial analysis (Reich et al., 2006; Hanks et al., 2015; Hughes and Haran, 2013; Hefley et al., 2017; Adin et al., 2023; Briz-Redón, 2023). This approach, usually involving a method known as restricted spatial regression, dominated the literature as well as practical implementations for many years, but has since been shown to be problematic for several reasons (Khan and Calder, 2022; Zimmerman and Ver Hoef, 2022; Bradley, 2024). (iv) Research based on causal inference approaches (Thaden and Kneib, 2018; Papadogeorgou et al., 2019; Schnell and Papadogeorgou, 2020), an overview of which is in Reich et al. (2021).

Although this work has shed more light on spatial confounding, results appear at times to be counter-intuitive or mutually conflicting. This is in part because the complexity of spatial models means that conclusions are often based on simulation studies, potentially sensitive to the specific simulation setup. Moreover, the research direction (iii) above has led to a focus on the difference between the estimates in the spatial and non-spatial analyses for identifying confounding bias. However, as our results confirm, this difference does not in itself determine whether either estimate is biased.

We develop a theoretical framework that brings mathematical clarity to the mechanisms of spatial confounding and the methods used for dealing with the resulting bias. We show that it is a problem for spatial models in general, directly linked to spatial smoothing (in line with work on bias in linear mixed models, Schnell and Bose, 2019). Central to our findings is the analytical expression for the bias derived in Proposition 1 which shows that, in the metric defined by the precision matrix of the chosen spatial analysis model, the bias is *the correlation between the covariate and the confounder times the size of the confounder relative to the size of the covariate*. Not only is this an intuitive result, but by using an eigendecomposition of the precision matrix, we derive a nuanced and detailed understanding of how the bias depends on the underlying confounding scenario and the covariance structure and parameters of the analysis model. This includes a deepened understanding of the role of spatial frequencies, defined directly in terms of the analysis model and the resulting eigendecomposition. While the expression for the bias is itself relatively simple to derive and aligns with earlier results on regularized regression, the dependence on individual components and parameters in the spatial context is complex, explaining the subtle and at times counter-intuitive behaviours. We illustrate our findings in a simulation study of several different scenarios.

A number of recent works (Dupont et al., 2022; Gilbert et al., 2024; Bolin and Wallin, 2024) have investigated the asymptotic behaviour of the covariate effect estimate in models of the form (1) under infill asymptotics, in particular, Gilbert et al. (2024) and Dupont et al. (2022) show that if the covariate has non-spatial information, the bias tends to zero as the sample size goes to infinity. Of course, in

practice, this limit is never reached. Our focus in this paper is on the behaviour of the covariate effect estimate in (1) for a finite sample size. We show that, in this case, there are scenarios in which spatial confounding bias is negligible (in line with Khan and Berrett (2023)), however, there are also scenarios in which the bias can become arbitrarily large.

Based on our results, we develop a general framework for assessing and adjusting spatial confounding bias in practice, applicable under any specification of the spatial effects in (1). The proposed method depends on whether or not the covariate has non-spatial information. When non-spatial information is present, we show that a general form of spatial+ (Dupont et al., 2022) can be used to eliminate bias. When no such information is present, the situation is more challenging as further assumptions for identifiability are needed. Under the assumption of unconfounded high frequencies (as proposed in Guan et al. (2023)), we develop a method that utilises the spatial frequency behaviours of the covariate to assess the bias in this case. Specifically, we propose a procedure in which multiple capped versions of spatial+ are applied. The method can easily be adapted to the scenario in which other frequencies than the highest ones are assumed to be unconfounded.

We illustrate our approach with an application to monthly mean air temperature across Germany during the year 2010 with rainfall as covariate. Both variables display varying spatial frequency behaviours for different months of the year. We show how our methods can be applied to assess whether the effect estimate in the spatial model is biased and, if so, determine the estimated bias.

In the following, we first establish some preliminary results on spatial regression models in Section 2 that will allow us to derive compact and intuitive expressions for bias arising due to spatial confounding in Section 3, supplemented by detailed simulations in Section 4. In Section 5, we propose a method for assessing bias in practice, supplemented by an illustrative simulation study. Finally, in Section 6, we illustrate our approach with an application.

## 2 Definitions and preliminary results

### 2.1 Model specification

Throughout this paper we assume that the true data generating process is given by

$$\mathbf{y} = \beta \mathbf{x} + \mathbf{z} + \boldsymbol{\epsilon}, \quad \boldsymbol{\epsilon} \sim N(\mathbf{0}, \sigma^2 \mathbf{I}) \quad (2)$$

where  $\mathbf{y} = (y(s_1), \dots, y(s_n))^T$ ,  $\mathbf{x} = (x(s_1), \dots, x(s_n))^T$  and  $\boldsymbol{\epsilon} = (\epsilon(s_1), \dots, \epsilon(s_n))^T$  are the response, covariate and error term at locations  $s_1, \dots, s_n$  and  $\mathbf{z} = (z(s_1), \dots, z(s_n))^T$  the true confounding variable at these locations. Since the confounder is assumed to be unknown, in the spatial analysis model chosen by the researcher analysing the data, we assume that  $\mathbf{z}(s)$  is approximated by a spatial effect  $\gamma(s)$  as in (1). This implies an analysis model of the form

$$\mathbf{y} = \beta \mathbf{x} + \mathbf{B}_{\text{sp}} \boldsymbol{\beta}_{\text{sp}} + \boldsymbol{\epsilon}, \quad \boldsymbol{\beta}_{\text{sp}} \sim N(\mathbf{0}, \lambda^{-1} \mathbf{S}^-), \quad \boldsymbol{\epsilon} \sim N(\mathbf{0}, \sigma^2 \mathbf{I}) \quad (3)$$

where  $\mathbf{B}_{\text{sp}}$  is an  $n \times p$  design matrix for the basis representing the spatial effect  $\gamma(s)$ , and  $\boldsymbol{\beta}_{\text{sp}}$  the coefficients for the spatial effect in this basis. The matrix  $\mathbf{S}$  (with pseudo-inverse  $\mathbf{S}^-$ ) is a  $p \times p$  penalty matrix which, together with the spatial basis in the design matrix  $\mathbf{B}_{\text{sp}}$ , defines the structure of the spatial effect, and  $\lambda > 0$  is a smoothing parameter which controls the overall level of smoothing of the spatial effect. If the model matrix is identifiable (a discussion of this is in Section 5), we can also allow the value  $\lambda = 0$ , in which case the spatial random effect becomes unsmoothed additional fixed effect terms in the model. We assume that  $\mathbf{S}$  is symmetric positive semi-definite, i.e. it has non-negative eigenvalues  $\alpha_1 \leq \dots \leq \alpha_p$ . The null space of  $\mathbf{S}$ , which could be non-trivial, corresponds to unsmoothed spatial vectors. The intercept in model (3) is not included as a separate fixed effect, as it can be modelled as part of the spatial effect by including the vector  $(1, \dots, 1)^T$  as an unpenalised spatial basis vector in  $\mathbf{B}_{\text{sp}}$ .

For comparison, we also consider the non-spatial analysis model

$$\mathbf{y} = \beta_0 + \beta \mathbf{x} + \boldsymbol{\epsilon}, \quad \boldsymbol{\epsilon} \sim N(\mathbf{0}, \sigma^2 \mathbf{I}) \quad (4)$$

where  $\beta_0 \in \mathbb{R}$  is an unknown intercept.

Owing to the generality of our setup, all the commonly used spatial models fit into this generic framework. For example, for (i) Gaussian random fields based on coordinate information,  $\mathbf{B}_{sp}$  is an incidence matrix linking observations to observation locations and  $\mathbf{S}$  is the inverse covariance matrix implied by the covariance function (ii) (intrinsic) conditional auto-regressive and Gaussian Markov random field specifications for regional data,  $\mathbf{B}_{sp}$  is an indicator matrix for the regions and  $\mathbf{S}$  encodes spatial proximity with an adjacency matrix or graph Laplacian, and (iii) tensor product P-splines and thin plate splines,  $\mathbf{B}_{sp}$  contains basis function evaluations and  $\mathbf{S}$  the corresponding smoothness penalty. We can also take a Bayesian perspective if we have a multivariate Gaussian prior on  $\beta_{sp}$  with precision  $\lambda \mathbf{S}$ , see Fahrmeir and Kneib (2011) for details on both the various options for spatial smoothing and the Bayesian perspective on spatial regression.

## 2.2 The spatial precision matrix $\Sigma^{-1}$

Central to our further analyses are the properties of the precision matrix  $\Sigma^{-1}$  of the spatial analysis model (3), derived from the covariance structure  $\Sigma = \sigma^2 \mathbf{I} + \lambda^{-1} \mathbf{B}_{sp} \mathbf{S}^{-1} \mathbf{B}_{sp}^T$ . Details of our derivations are included in Appendix 1.1. The following lemma shows how the eigenvectors of  $\Sigma^{-1}$  are linked to the penalisation (i.e. the spatial smoothing) in the chosen analysis model.

**Lemma 1** *Let  $\alpha_1 \leq \dots \leq \alpha_p$  be the eigenvalues of the penalty matrix  $\mathbf{S}$  and  $\lambda > 0$  the smoothing parameter. Then the eigenvalues of the precision matrix  $\Sigma^{-1}$  are given by  $\{\sigma^{-2}, \sigma^{-2}w_1, \dots, \sigma^{-2}w_p\}$  where  $w_i = \lambda\alpha_i/(\sigma^{-2} + \lambda\alpha_i)$  for  $i = 1, \dots, p$ .*

Using this result, we obtain a natural decomposition of the sample space  $\mathbb{R}^n$ . Specifically, Lemma 1 shows that there exists an  $n \times n$ -matrix  $\mathbf{U}$  such that

$$\mathbf{U}^T \Sigma^{-1} \mathbf{U} = \sigma^{-2} \text{diag}(1, \dots, 1, w_1, \dots, w_p),$$

where  $w_i = \lambda\alpha_i/(\sigma^{-2} + \lambda\alpha_i)$  for  $i = 1, \dots, p$ , and the columns of  $\mathbf{U}$  form an orthonormal basis of eigenvectors in  $\mathbb{R}^n$ . As elements of the sample space, each of the eigenvectors represent different behaviours over the spatial domain. The first  $n - p$  eigenvectors  $\mathbf{U}_{ns}$  have eigenvalue  $\sigma^{-2}$  and are unaffected by smoothing. Therefore, the subspace spanned by these can be considered as the “non-spatial” part of the sample space. The remaining  $p$  eigenvectors  $\mathbf{U}_{sp}$  represent the spatially smoothed behaviours, where the  $i$ th eigenvector has eigenvalue  $\sigma^{-2}w_i$  with  $w_i$  a weight between 0 and 1, directly linked to the  $i$ th smoothing penalty  $\alpha_i$ . Although, the values of the weights depend on the parameters  $\sigma^{-2}$  and  $\lambda$ , which are usually estimated, the eigenvectors do not. Moreover, irrespective of the parameter estimates, the ordering of the weights is the same as the  $\alpha_i$ ’s, i.e.

$$0 \leq w_1 \leq \dots \leq w_p \leq 1.$$

Thus, spatial eigenvectors with weights close to 1 correspond to behaviours that are penalised more, i.e. that are considered “less spatial” according to the analysis model. We will therefore refer to behaviours given by eigenvectors with high weights  $w_i$  as “high frequency” and eigenvectors with low weights  $w_i$  as “low frequency”. For further details, see Appendix 1.2.

Although spatial frequencies are generally known to play an important role for spatial confounding, there is no single definition in the literature for what is meant by spatial frequencies (see Appendix 1.2). Describing them directly through the eigenvectors of the spatial precision matrix  $\Sigma^{-1}$  has several advantages:

- For any choice of analysis model (3), these eigenvectors are well-defined and can be easily computed, even when the dimension  $p$  of the spatial effect is smaller than the sample size  $n$ ;
- The eigenvectors form an orthonormal basis for the  $n$ -dimensional sample space;
- The eigenvectors are directly and quantifiably linked to the penalisation (i.e. spatial smoothing) in the chosen analysis model (as set out in Lemma 1).

Thus, what is considered high/low frequency spatial behaviour is always well-defined and determined by the spatial structure chosen for the spatial analysis model.

Finally, since the precision matrix  $\Sigma^{-1}$  is symmetric positive definite it defines an inner product on  $\mathbb{R}^n$ . For the rest of this paper, if  $\mathbf{M}$  is a symmetric positive definite  $n \times n$  matrix, we will use the notation  $\langle \cdot, \cdot \rangle_{\mathbf{M}}$  to denote the inner product defined by  $\mathbf{M}$  and  $\|\cdot\|_{\mathbf{M}}$  the corresponding norm. That is,  $\langle \mathbf{v}, \mathbf{v}' \rangle_{\mathbf{M}} = \mathbf{v}^T \mathbf{M} \mathbf{v}'$  and  $\|\mathbf{v}\|_{\mathbf{M}} = \sqrt{\langle \mathbf{v}, \mathbf{v} \rangle_{\mathbf{M}}}$  for all  $\mathbf{v}, \mathbf{v}' \in \mathbb{R}^n$ .

### 3 Characterising the impact of spatial confounding

In this section, Proposition 1 and Corollary 1 provide explicit expressions for the bias of the covariate effect estimate in the analysis model (3) arising from spatial confounding. We assume throughout that the true data generating process is that of model (2) with true covariate effect  $\beta$  and true spatial confounder  $\mathbf{z}$ , where the latter is assumed to be generated from the spatial structure of model (3). Thus, our results do not rely on model mis-specification; the bias occurs even when the analysis model is perfectly able to reproduce the confounder. Further bias could arise when the analysis model is mis-specified, but this is not our focus here.

#### 3.1 Bias in the spatial model

**Proposition 1** The bias of the estimated covariate effect  $\hat{\beta}$  in model (3) is given by

$$E(\hat{\beta}) - \beta = \frac{\langle \mathbf{x}, \mathbf{z} \rangle_{\Sigma^{-1}}}{\langle \mathbf{x}, \mathbf{x} \rangle_{\Sigma^{-1}}} = \frac{\langle \mathbf{x}, \mathbf{z} \rangle_{\Sigma^{-1}}}{\|\mathbf{x}\|_{\Sigma^{-1}} \|\mathbf{z}\|_{\Sigma^{-1}}} \frac{\|\mathbf{z}\|_{\Sigma^{-1}}}{\|\mathbf{x}\|_{\Sigma^{-1}}}.$$

Thus, the bias has the intuitive interpretation as the correlation between  $\mathbf{x}$  and  $\mathbf{z}$  times the size of  $\mathbf{z}$  relative to the size of  $\mathbf{x}$  in the metric defined by  $\Sigma^{-1}$ . That is, in this metric, the bias gets large exactly when the covariate and the confounder are very correlated *and* the confounder is relatively large compared to the covariate. The sign of the bias is the same as the sign of the correlation, i.e. the sign of  $\langle \mathbf{x}, \mathbf{z} \rangle_{\Sigma^{-1}}$ . The proof of the proposition is in Appendix 1.3.

Combining Proposition 1 with the results of Section 2 we get a better understanding of how the bias behaves. Let  $\xi^x = (\xi_{ns}^{xT}, \xi_{sp}^{xT})^T$  denote the coordinates of  $\mathbf{x}$  in the eigenbasis  $\mathbf{U}$  such that  $\mathbf{x} = \mathbf{U} \xi^x$ , i.e. a non-zero entry in  $\xi^x$  means that the corresponding basis vector is included in  $\mathbf{x}$ . Similarly, let  $\mathbf{z} = \mathbf{U} \xi^z$ . Since  $\mathbf{z}$  is spatial,  $\xi_{ns}^z = \mathbf{0}$ . It is now straightforward to prove the following result (see Appendix 1.4. for the proof).

**Corollary 1** Let  $\mathbf{U}$  be the orthonormal eigenbasis which diagonalises  $\Sigma^{-1}$ , and  $\xi^x = (\xi_{ns}^{xT}, \xi_{sp}^{xT})^T$  and  $\xi^z = (\mathbf{0}^T, \xi_{sp}^{zT})^T$  the coordinates of  $\mathbf{x}$  and  $\mathbf{z}$  in this basis. The bias of the estimated covariate effect  $\hat{\beta}$  in model (3) is given by

$$E(\hat{\beta}) - \beta = \frac{\sum_{i=1}^p \xi_{sp,i}^x \xi_{sp,i}^z w_i}{\sum_{i=1}^{n-p} (\xi_{ns,i}^x)^2 + \sum_{i=1}^p (\xi_{sp,i}^x)^2 w_i},$$

where  $w_i = \lambda \alpha_i / (\sigma^{-2} + \lambda \alpha_i)$  for  $i = 1, \dots, p$ .

The expression in Corollary 1 (consistent with (10) of Schnell and Bose (2019)) shows that bias in the spatial model is directly linked to spatial smoothing, as without smoothing (i.e. if  $\alpha_i = 0$  for all  $i$  or  $\lambda = 0$ ), the bias would not arise. In other words, adding spatial random effects to the model (4) adjusts for unmeasured spatial confounders thereby, in principle, eliminating bias, however, bias is reintroduced as a result of spatial smoothing. For any given  $\lambda > 0$ , i.e. a fixed overall level of smoothing, we see that bias occurs whenever  $\mathbf{x}$  and  $\mathbf{z}$  share a spatial component for which  $w_i \neq 0$ . More specifically, any confounded component in  $\mathbf{x}$ , i.e. with  $\xi_{\text{sp},i}^x \xi_{\text{sp},i}^z \neq 0$ , contributes to the numerator of the bias. At the same time, all components in  $\mathbf{x}$  increase the denominator, thereby reducing the overall size of the bias.

The expression for the bias is not symmetric in  $\mathbf{x}$  and  $\mathbf{z}$ . In particular, it is not affected by components in  $\mathbf{z}$  for which the corresponding component in  $\mathbf{x}$  is 0 (i.e. when  $\xi_{\text{sp},i}^z \neq 0$  but  $\xi_{\text{sp},i}^x = 0$ ). Thus, any unmeasured spatial variation in the response variable that is independent of the covariate can be ignored for the purposes of the bias. However, such components may affect the overall fit of the model and the estimates of the parameters  $\lambda$  and  $\sigma^2$  which affect the weights  $w_i$ .

### 3.2 The role of spatial frequencies

Due to the differences in the weights  $w_i$ , different spatial frequencies affect the bias differently.

Looking at the numerator in Corollary 1, any confounded spatial component of  $\mathbf{x}$  (i.e. those with  $\xi_{\text{sp},i}^x \neq 0$  and  $\xi_{\text{sp},i}^z \neq 0$ ) contribute to the bias, and the larger the weight, the larger the contribution. So confounding at high frequencies (where weights are close to 1) induce larger bias, while confounding at low frequencies may give a negligible contribution. Confounding at unpenalised spatial frequencies does not lead to bias (as they have weights 0), and non-spatial components in  $\mathbf{x}$  do not contribute to the numerator either. For all confounded frequencies in  $\mathbf{x}$  with  $w_i \neq 0$ , the contribution to the bias is proportional to the size  $\xi_{\text{sp},i}^z$  of the confounder at that frequency. Contributions to the bias from different eigenvectors can partially cancel each other out as they can have different signs.

From the denominator we see that any unconfounded components of  $\mathbf{x}$ , that is, either non-spatial components  $\xi_{\text{ns},i}^x \neq 0$  or spatial components with  $\xi_{\text{sp},i}^x \neq 0$  and  $\xi_{\text{sp},i}^z = 0$ , will reduce the size of the bias, as they increase the denominator without affecting the numerator. This reduction will be larger when the weight  $w_i$  is large, i.e. when the spatial frequency is high, and may be negligible or even 0 for low frequencies. Unconfounded high frequency spatial components of  $\mathbf{x}$  have a similar effect on the bias as non-spatial components (in line with the intuition that high frequencies are ‘‘less spatial’’), i.e. they contribute nothing to the numerator and are included with weight close to 1 in the denominator.

### 3.3 Comparison to the non-spatial model

Irrespective of the size of bias, the non-spatial model (4) is not an appropriate analysis model for the data generation process (2), as the residual spatial variation in the response data violates the assumptions of the model. Indeed, this is the reason for including spatial random effects. Nevertheless, we consider how the bias in model (4) compares to the spatial model (3) as this has been a focus of spatial confounding research in the past. The following corollary is proved in Appendix 1.8.

**Corollary 2** *Let  $\mathbf{U}$  be the orthonormal eigenbasis which diagonalises  $\Sigma^{-1}$ , and  $\xi^x = (\xi_{\text{ns}}^{xT}, \xi_{\text{sp}}^{xT})^T$  and  $\xi^z = (\mathbf{0}^T, \xi_{\text{sp}}^{zT})^T$  the coordinates of  $\mathbf{x}$  and  $\mathbf{z}$  in this basis. The bias of the estimated covariate effect  $\hat{\beta}_{\text{ns}}$  in model (4) is given by*

$$E(\hat{\beta}_{\text{ns}}) - \beta = \frac{\langle \mathbf{x}, \mathbf{z} \rangle}{\langle \mathbf{x}, \mathbf{x} \rangle} = \frac{\langle \mathbf{x}, \mathbf{z} \rangle}{\|\mathbf{x}\| \|\mathbf{z}\|} \frac{\|\mathbf{z}\|}{\|\mathbf{x}\|} = \frac{\sum_{i=1}^p \xi_{\text{sp},i}^x \xi_{\text{sp},i}^z}{\sum_{i=1}^{n-p} (\xi_{\text{ns},i}^x)^2 + \sum_{i=1}^p (\xi_{\text{sp},i}^x)^2}.$$

Thus, the bias in the non-spatial model differs to that of the spatial model only in that all spatial frequencies have weights 1 rather than  $w_i$ . Broadly speaking, bias in the non-spatial model reflects the

overall correlation between  $\mathbf{x}$  and  $\mathbf{z}$ , whereas bias in the spatial model depends mostly on the correlation at high frequencies. However, as the weights affect both the numerator and denominator of the bias, in general, the relationship between the two models is not straightforward. A detailed computation of the difference and how it is affected by different types of behaviours is given in Appendix 1.4. Although the bias tends to be larger in the non-spatial model than in the spatial model, there are scenarios where it is the other way around.

In the past, the estimate in model (4) was often mistakenly assumed to be unbiased and, therefore, a large difference between this and the estimate in (3) was seen as a sign of confounding bias in the spatial model (and, conversely, a small difference a sign of no confounding). However, Corollary 2 shows that a difference between these estimates tends to arise when the covariate is dominated by low frequencies (as these have weights most different from 1) and the existence of such a difference does not necessarily mean that there is confounding bias in the spatial model. Conversely, we see that if the covariate is dominated by high frequencies (with weights close to 1), the estimates in the two models will be similar, but this does not necessarily mean that they are unbiased.

### 3.4 Dependence on the smoothing parameter

As bias in the spatial model is caused by smoothing, intuitively, we would expect larger values of the parameter  $\lambda$  to lead to more bias when all other components are held fixed. However, as  $\lambda$  affects both the numerator and the denominator of the expression in Corollary 1, there can be situations where this is not the case. In Appendix 1.5 we provide a detailed analysis which shows that, although the behaviour of the bias varies, when there is sufficient non-spatial or unconfounded high frequency components in  $\mathbf{x}$ , the size of the bias broadly increases with  $\lambda$  (in line with intuition). The following corollary is also proved in the Appendix 1.6.

**Corollary 3** *Let  $\mathbf{U}$  be the orthonormal eigenbasis which diagonalises  $\Sigma^{-1}$ , and  $\xi^x = (\xi_{ns}^{xT}, \xi_{sp}^{xT})^T$  and  $\xi^z = (\mathbf{0}^T, \xi_{sp}^{zT})^T$  the coordinates of  $\mathbf{x}$  and  $\mathbf{z}$  in this basis. The bias of the estimated covariate effect  $\hat{\beta}$  in model (3) has the following limiting behaviour:*

$$\begin{aligned} \lim_{\lambda \rightarrow 0} E(\hat{\beta}) - \beta &= \begin{cases} 0 & \text{if } \xi_{ns}^x \neq \mathbf{0} \\ \frac{\sum_{i=1}^p \xi_{sp,i}^x \xi_{sp,i}^z \alpha_i}{\sum_{i=1}^p (\xi_{sp,i}^x)^2 \alpha_i} & \text{otherwise} \end{cases} \\ \lim_{\lambda \rightarrow \infty} E(\hat{\beta}) - \beta &= \frac{\sum_{\{i|\alpha_i \neq 0\}} \xi_{sp,i}^x \xi_{sp,i}^z}{\sum_{i=1}^{n-p} (\xi_{ns,i}^x)^2 + \sum_{\{i|\alpha_i \neq 0\}} (\xi_{sp,i}^x)^2}. \end{aligned}$$

Thus, in the limit  $\lambda \rightarrow \infty$ , i.e. an entirely smoothed spatial effect, the bias in the spatial model agrees with that of the non-spatial model, except that any contributions from unpenalised spatial components of  $\mathbf{x}$  are 0. In the limit  $\lambda \rightarrow 0$ , i.e. without smoothing, the behaviour of the bias depends on whether or not the covariate has non-spatial information. If non-spatial information is present, the bias can be eliminated by setting  $\lambda = 0$ , though this is usually undesirable as it is likely lead to an inferior model fit. Similarly, if the proportion of unconfounded high frequency components in  $\mathbf{x}$  is large, then the size of the bias reduces as  $\lambda \rightarrow 0$  and the limit is close to 0. But in the absence of non-spatial or unconfounded high frequency information, the limit could become large and even exceed the bias of the non-spatial model.

## 4 Simulation studies

In the following sections we simulate different confounding scenarios to study the behaviour of the bias of the covariate effect estimate  $\hat{\beta}$  in model (3) and  $\hat{\beta}_{ns}$  in model (4). For each scenario we generate 100

independent replicates of covariate data  $\mathbf{x}$  and response data  $\mathbf{y}$ , observed at  $n = 1000$  randomly selected locations in the spatial domain  $[0, 1] \times [0, 1] \subset \mathbb{R}^2$  such that

$$\mathbf{y} = \beta \mathbf{x} + \mathbf{z} + \boldsymbol{\epsilon}^y, \quad \mathbf{x} = \mathbf{z}^x + \boldsymbol{\epsilon}^x$$

where  $\beta \in \mathbb{R}$ ,  $\boldsymbol{\epsilon}^y \sim N(\mathbf{0}, \sigma^2 \mathbf{I})$ ,  $\boldsymbol{\epsilon}^x \sim N(\mathbf{0}, \sigma_x^2 \mathbf{I})$  for  $\sigma, \sigma_x > 0$ . In this specification,  $\mathbf{z}$  and  $\mathbf{z}^x$  are constructed as linear combinations of two spatial fields  $\mathbf{z}_{\text{sp},l}$  and  $\mathbf{z}_{\text{sp},h}$ , which are low and high frequency, respectively, i.e.

$$\mathbf{z} = \xi_{\text{sp},l}^z \mathbf{z}_{\text{sp},l} + \xi_{\text{sp},h}^z \mathbf{z}_{\text{sp},h}, \quad \mathbf{z}^x = \xi_{\text{sp},l}^x \mathbf{z}_{\text{sp},l} + \xi_{\text{sp},h}^x \mathbf{z}_{\text{sp},h}$$

for  $\xi_{\text{sp},l}^z, \xi_{\text{sp},h}^z, \xi_{\text{sp},l}^x, \xi_{\text{sp},h}^x \in \mathbb{R}$ , while  $\boldsymbol{\epsilon}^x$  is spatially unstructured and represents the non-spatial component of  $\mathbf{x}$ . Unless stated otherwise, we let  $\beta = 0.5$ ,  $\sigma_x = \sigma = 1$ .

For the regressions in this section, we represent the spatial effect as a thin plate regression spline (TPRS), a computationally efficient reduced rank version of a thin plate spline (Wood, 2003). The data generating process matches the analysing spatial model which is therefore correctly specified. In Appendix 4, we repeat the simulation where the data generating process is a Gaussian process, so in addition to the spatial confounding bias, there may be further mis-specification bias. In order to generate  $\mathbf{z}_{\text{sp},l}$  and  $\mathbf{z}_{\text{sp},h}$ , we start by considering a mean-zero Gaussian process  $\gamma$  with exponential covariance structure following  $C(h) = \exp(-h/\kappa)$  such data  $h = \|\mathbf{s} - \mathbf{s}'\|$  for  $\mathbf{s}, \mathbf{s}' \in [0, 1] \times [0, 1]$ , which is assumed for simplicity to have variance of 1. We set  $\kappa = 0.1$  corresponding to a spatial range of approximately 0.3. We fit thin plate regression splines to the generated  $\gamma$  with 10 and 800 basis functions, respectively, and use the corresponding fitted values as  $\mathbf{z}_{\text{sp},l}$  and  $\mathbf{z}_{\text{sp},h}$ . Thin plate regression spline models are implemented in the R-package mgcv. We use this implementation with generalised cross-validation as the smoothness selection criterion to compare the results of models fitted to simulated data for which we know the true underlying covariate and spatial dependence. We consider 600 basis functions for the thin plate regression splines in the data analysing model.

## 4.1 Scenario 1: Confounding at high frequencies

From Corollary 1 we expect confounding at high frequencies, i.e.  $\xi_{\text{sp},h}^x \xi_{\text{sp},h}^z \neq 0$ , to lead to bias in the spatial model. The larger the value of  $\xi_{\text{sp},h}^x \xi_{\text{sp},h}^z$ , the larger the numerator in the bias. In fact, keeping everything else fixed, the bias increases linearly with  $\xi_{\text{sp},h}^z$  and can therefore become arbitrarily large. From Corollary 2 we expect the same behaviour in the non-spatial model, as the bias has the same expression as that of the spatial model, except that each weight  $w_i$  is replaced by 1. Thus, we consider  $(\xi_{\text{sp},l}^x, \xi_{\text{sp},h}^x) = (1, 1)$ ,  $\xi_{\text{sp},l}^z = 0$  and  $\xi_{\text{sp},h}^z \in \{0.2, 0.5, 1\}$ .

As expected, Figure 1 (top left) shows significant bias in both models under this scenario, increasing linearly in size with  $\xi_{\text{sp},h}^z$ . The mean squared error (MSE) of fitted values compared to the true expectation of  $\mathbf{y}$  is shown in Appendix 3.1 and is always lower for the spatial model, indicating a better fit, which is not surprising as the spatial model is correctly specified, whereas the non-spatial model is mis-specified.

## 4.2 Scenario 2: Confounding at low frequencies

We reconsider Scenario 1 but with high and low frequencies swapped, i.e.  $(\xi_{\text{sp},l}^x, \xi_{\text{sp},h}^x) = (1, 1)$ ,  $\xi_{\text{sp},h}^z = 0$  and  $\xi_{\text{sp},l}^z \in \{0.2, 0.5, 1\}$ . Since confounding is now at low frequencies, i.e.  $\xi_{\text{sp},l}^x \xi_{\text{sp},l}^z \neq 0$ , contributions to the numerator of the bias in the spatial model are multiplied by low weights  $w_i$ , while the denominator of the bias is still relatively large due to the non-spatial information in  $\mathbf{x}$ . Therefore we expect the bias to be small. This is confirmed in the results shown in Figure 1 (top right) where the bias in the spatial model remains close to zero, even when  $\xi_{\text{sp},l}^z$  is increased. In contrast, swapping frequencies makes no difference to the non-spatial model as all frequencies have equal weight and, indeed, the behaviour for this model is the same as in Scenario 1. Appendix 3.1 confirms, as before, that the spatial model is superior in terms of fit.

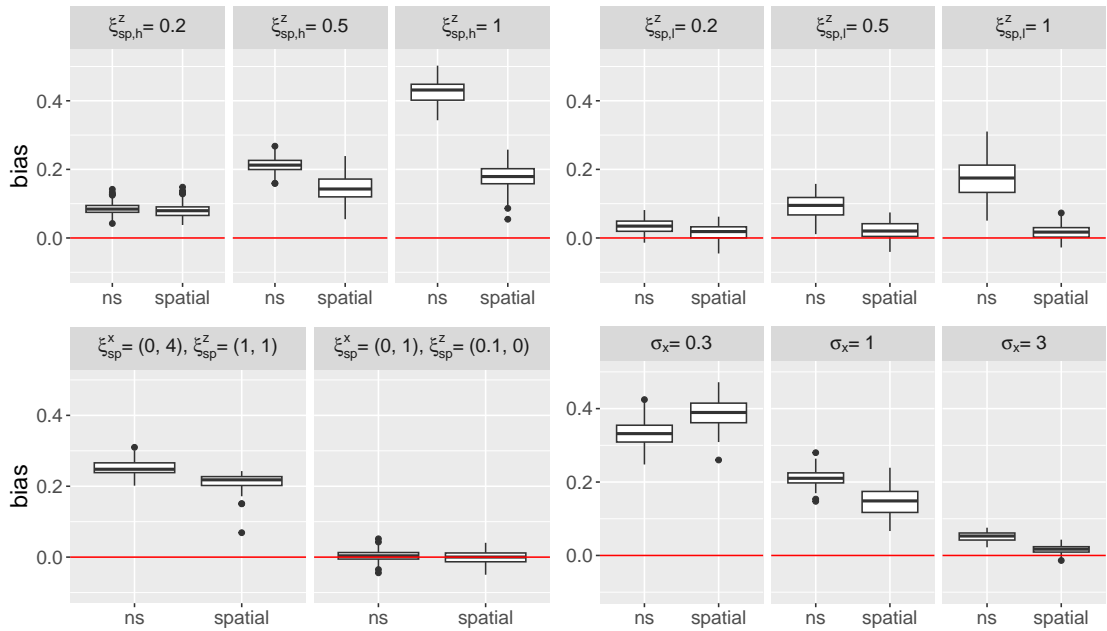


Figure 1: Bias of  $\hat{\beta}$  and  $\hat{\beta}_{ns}$  in the spatial and non-spatial (ns) models under Scenario 1 (top, left), Scenario 2 (top, right), Scenario 3 (bottom, left), Scenario 4 (bottom, right). The true value of  $\beta$  is 0.5.

### 4.3 Scenario 3: Comparison to the non-spatial model

In Section 3.3 we noted that difference or similarity between the estimates in the spatial and non-spatial models cannot in itself be used to diagnose the existence or otherwise of bias in the spatial model. This is illustrated in Scenarios 1 and 2 above, as in both of these scenarios the estimates in the two models differ but, in Scenario 1, the spatial model is biased whereas, in Scenario 2, it is not. To illustrate this point further, here we simulate two scenarios in which the estimates in the two models are similar, but in one scenario both models are biased whereas in the other they are both largely unbiased. Specifically, in order to generate  $\mathbf{z}_{sp,h}$  and  $\mathbf{z}_{sp,l}$ , we fit a reparametrised TPRS spatial effect (see Appendix 2) to the Gaussian process with  $\kappa = 0.1$  where the corresponding 75 highest frequencies are used to generate  $\mathbf{z}_{sp,h}$  and the remaining frequencies to generate  $\mathbf{z}_{sp,l}$ . We consider: (1) biased scenario with  $(\xi_{sp,l}^x, \xi_{sp,h}^x) = (0, 4)$  and  $(\xi_{sp,l}^z, \xi_{sp,h}^z) = (1, 1)$ ; (2) unbiased scenario with  $(\xi_{sp,l}^x, \xi_{sp,h}^x) = (0, 0.1)$  and  $(\xi_{sp,l}^z, \xi_{sp,h}^z) = (1, 0)$ . We use  $n$  basis functions in the the data analysis model. In the first scenario,  $\mathbf{x}$  has only high frequencies which are all confounded, so the spatial model is biased with weights  $w_i$  close to 1, making the bias similar to that of the non-spatial model. In the second scenario, there are no overlapping frequencies between  $\mathbf{x}$  and  $\mathbf{z}$  so both models are unbiased. The results are shown in Figure 1 (bottom, left).

Section 3.3 also showed that while the bias in the non-spatial model tends to exceed that of the spatial model, it could also be the other way around. In both Scenarios 1 and 2, the bias in the non-spatial model always stays above the spatial model bias. However, in Appendix 3.2, we repeat Scenario 1 with a larger proportion of unconfounded low frequency components in  $\mathbf{x}$  so that the correlation between  $\mathbf{x}$  and  $\mathbf{z}$  is low overall, but high at high frequencies. As expected from our analysis, in this latter scenario, the bias in the spatial model exceeds that of the non-spatial model.

## 4.4 Scenario 4: Dependence on non-spatial information

We now study the effect on the bias of non-spatial information in the covariate  $\mathbf{x}$  by increasing the parameter  $\sigma_x$ . As the coefficient  $\xi_{\text{ns}}^x$  appears only in the denominator of the bias in both the spatial and non-spatial models, we expect bias in both models to reduce. Specifically, we consider  $\sigma_x \in \{0.3, 1, 3\}$ . Other parameters remain constant at  $(\xi_{\text{sp},l}^x, \xi_{\text{sp},h}^x) = (1, 1)$ ,  $(\xi_{\text{sp},l}^z, \xi_{\text{sp},h}^z) = (0, 0.5)$ .

Figure 1 (bottom, right) shows that, as expected, the bias decreases for both models when  $\sigma_x$  is increased, and the case  $\sigma_x = 3$  illustrates that, for a sufficiently large non-spatial component of  $\mathbf{x}$ , the bias in the spatial model becomes negligible. As before, the MSE of fitted values is always larger for the non-spatial model. In Section 3.3, we saw that bias in the non-spatial model tends to exceed that of the spatial model, but if the covariate has little non-spatial information and confounding takes place at high frequencies, then it may be the other way around. This behaviour is observed in Figure 1 where the bias in the non-spatial model is higher than that of the spatial model, except in the case  $\sigma_x = 0.3$ , i.e where  $\mathbf{x}$  has the smallest amount of non-spatial information.

## 4.5 Scenario 5: Dependence on the smoothing parameter

As detailed in Section 3, the expression for the bias in the spatial model has a relatively complex dependency on the smoothing parameter  $\lambda$ . However, when there are sufficient non-spatial or unconfounded high frequency components in  $\mathbf{x}$ , we expect the bias to broadly increase from zero and, assuming there are not many unpenalised spatial components in  $\mathbf{x}$ , eventually approach the bias in the corresponding non-spatial model. Here, we simulate this type of data under three data generation processes, chosen to broadcast a range of behaviours. The simulated data has confounding at high frequencies, unconfoundedness at low frequencies and varying amounts of non-spatial information, specifically,  $\sigma_x \in \{0.3, 1, 2\}$ . We use 10 basis functions to generate  $\mathbf{z}_{\text{sp},l}$  and 800 basis functions for  $\mathbf{z}_{\text{sp},h}$ . Moreover, we let  $(\xi_{\text{sp},l}^x, \xi_{\text{sp},h}^x) = (1, 1)$ ,  $(\xi_{\text{sp},l}^z, \xi_{\text{sp},h}^z) = (0, 0.5)$  and fix  $\lambda$  at different values. We consider 20 replicates and compute the average spatial and non-spatial bias for those replicates using 800 basis functions in the analysing spatial model.

Figure 2 shows that for  $\sigma_x = 0.3$ , the spatial bias increases from 0, crosses that of the non-spatial model and stays above it, until they meet again for large  $\lambda$ . As expected, increasing non-spatial information in  $\mathbf{x}$  decreases bias in general, and for  $\sigma_x = 1$  and  $\sigma_x = 2$ , the bias of the spatial model stays below that of the non-spatial model. For each data generating process in Figure 2, we also show the median estimated smoothing parameter  $\hat{\lambda}$  using the generalised cross-validation criterion. At the estimated values of  $\lambda$  the bias is 0.4037, 0.1804 and 0.0362, from left to right. For  $\sigma_x = 0.3$ , the generalised cross-validation estimate is in a relatively flat area of the curve where the bias in the spatial model exceeds that of the non-spatial model. For both of the other values of  $\sigma_x$ , although the spatial model bias is bounded by the non-spatial model bias, the estimate  $\hat{\lambda}$  is at the steep part of the curve, which means that small changes in  $\hat{\lambda}$  can lead to large changes in the bias.

## 5 Bias adjustment

As the expressions in Section 3 involve the unknown confounder  $\mathbf{z}$ , in practical applications, we cannot simply compute the bias to assess the impact of confounding. Moreover, as illustrated in Section 3.3 and the Scenario 3 simulations above, the difference between the estimates in the spatial and non-spatial models is a poor diagnostic for the existence or otherwise of bias. Here, instead we propose a general framework for bias assessment and adjustment based on our results. That is, for a given data set and choice of spatial analysis model, we propose methods for estimating the bias under different assumptions for the data generation scenario. One assumption that is not usually highlighted in the spatial confounding literature is whether the covariate  $\mathbf{x}$  has non-spatial information. However, as illustrated in Sections 3 and

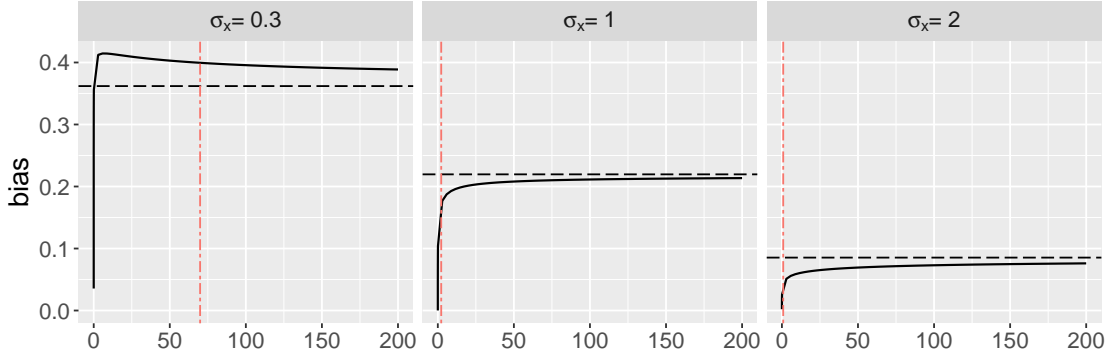


Figure 2: Bias of  $\hat{\beta}$  (solid black) and  $\hat{\beta}_{ns}$  (dashed black) for increasing  $\lambda$  and different  $\sigma_x$ . The true value of  $\beta$  is 0.5. The magenta dashed line shows the median  $\hat{\lambda}$  estimated by generalised cross-validation.

4, the bias may exhibit fundamentally different behaviour depending on whether or not this assumption holds. As outlined below, this assumption is also important in the context of bias adjustment.

### 5.1 Case 1: $\mathbf{x}$ has non-spatial information

If the covariate  $\mathbf{x}$  has non-spatial information, i.e.  $\xi_{ns}^x \neq 0$ , it means that, while the locations at which the data are collected induce some spatial dependency structure in the covariate data, there is additional variation that cannot be explained by the spatial information alone. In this case, the model matrix for (3) has full rank and the model is identifiable. Thus, the model has information to distinguish the effect of  $\mathbf{x}$  from that of  $\mathbf{z}$ , but bias in the covariate effect estimate arises as a result of distortion caused by spatial smoothing. If our only objective was to avoid the bias, we could simply remove or reduce the level of smoothing, indeed, Corollary 3 shows that the bias becomes zero as  $\lambda \rightarrow 0$ . However, undersmoothing is undesirable from the point of view of model fit, as smoothing is applied to reflect the spatial covariance structure and avoid overfitting the spatial effect.

Spatial+ (Dupont et al., 2022) is a method for bias adjustment which utilises the fact that the non-spatial component  $\mathbf{x}_{ns} = \mathbf{U}_{ns} \xi_{ns}^x$  of the covariate is unconfounded and can therefore be used to identify the covariate effect. Although originally introduced for models in which the spatial effect is a thin plate spline, the method can be formulated for any spatial analysis model as the following two-step procedure.

- (i) Fit the model (3) with no covariates to  $\mathbf{x}$  to obtain the decomposition  $\mathbf{x} = \mathbf{x}_{sp} + \mathbf{r}^x$  where  $\mathbf{x}_{sp}$  are the fitted values (estimating the spatial part of  $\mathbf{x}$ ) and  $\mathbf{r}^x$  the residuals.
- (ii) Estimate the covariate effect  $\beta$  by fitting the model (3) but with  $\mathbf{x}$  replaced by  $\mathbf{r}^x$ .

From Proposition 1, the bias in spatial+ is  $\langle \mathbf{r}^x, \mathbf{z} \rangle_{\Sigma^{-1}} / \langle \mathbf{r}^x, \mathbf{r}^x \rangle_{\Sigma^{-1}}$ . The residuals  $\mathbf{r}^x$  estimate the component  $\mathbf{x}_{ns}$  which lies in the non-spatial part of the sample space. As this subspace is orthogonal to the spatial part containing  $\mathbf{z}$ , this shows why we can expect the bias to be eliminated. Indeed, even though  $\mathbf{r}^x$  may contain a small proportion of potentially confounded spatial components, its non-spatial part is likely to dominate so that bias is negligible (as seen in the Scenario 4 simulations).

### 5.2 Case 2: $\mathbf{x}$ is fully spatial

Sometimes  $\mathbf{x}$  has no non-spatial components, i.e.  $\xi_{ns}^x = 0$ . For example,  $\mathbf{x}$  could be entirely generated from a smooth spatial process, or the dimension  $p$  of the spatial effect in (3) could be as large as the

sample size  $n$  (such as in a regional spatial model with one data measurement per region). The covariate vector is then contained in the space spanned by the spatial basis vectors and model (3) is unidentifiable. Here, the smoothing penalty not only improves the fit but acts as a regulariser. The model cannot be fitted without smoothing, and the apportionment of the covariate effect between the covariate and spatial terms of the model is directly related to how the smoothing is applied. Our expression for the bias still holds, however, unlike Case 1 above where the non-spatial component  $\mathbf{x}_{ns}$  is known to be unconfounded, we have no information of the confounding scenario and methods like spatial+ may not be effective. The behaviour of the bias will also generally be harder to predict. In particular, even if confounding is at low frequencies (making the numerator of the bias small), the bias could still be significant as the absence of non-spatial components in  $\mathbf{x}$  means that the denominator could also potentially be very small, especially when the covariate is dominated by low frequency behaviours.

As shown in Sections 3 and 4, spatial frequencies play a key role for the bias, and techniques such as Fourier and wavelet analysis are useful for understanding the behaviours of the observed variables  $\mathbf{y}$  and  $\mathbf{x}$  (as suggested, for example, in Keller and Szpiro (2020)). However, our expressions show that it is the frequencies shared by  $\mathbf{x}$  and  $\mathbf{z}$  that cause bias, and the data has no information on how such frequencies are split between the two variables. Therefore, without further (untestable) assumptions for identifiability, we cannot estimate the bias.

In the case where  $\mathbf{x}$  and  $\mathbf{z}$  are realisations of two stationary Gaussian spatial processes, Guan et al. (2023) use a Fourier transform to describe spatial frequencies and show that an assumption of unconfoundedness at high frequencies can be used to obtain identifiability. As noted in Guan et al. (2023), this assumption seems natural as the highest frequency spatial variation in a variable is more likely to be characteristic to that particular variable and therefore not confounded with other spatial variables. Corollary 1 shows that this idea extends to our framework in which spatial frequencies are defined directly in terms of the spatial analysis model (3) as described in Section 2.2. Unconfoundedness at the highest frequencies then corresponds to the assumption that  $\xi_{sp,i}^z = 0$  for frequencies above a certain threshold. Thus, under this assumption, the frequency components of  $\mathbf{x}$  above the threshold can be used to obtain identifiability.

We note that the frequencies used to obtain identifiability need not be the highest spatial frequencies. An example of this is the scenario of Bolin and Wallin (2024) who consider the asymptotic behaviour of the covariate effect estimate in an analysis model of the form (3) when the true data generation process is given by

$$\mathbf{y} = \beta \mathcal{S} \mathbf{x} + \boldsymbol{\epsilon}, \quad \boldsymbol{\epsilon} \sim N(\mathbf{0}, \sigma^2 \mathbf{I})$$

where  $\mathcal{S}$  is a smoothing operator, for example,  $\mathcal{S} \mathbf{x}$  could be the spatial frequencies of the covariate below a threshold  $k$  and  $\mathbf{x} - \mathcal{S} \mathbf{x}$  the remaining (higher) frequencies. Here, there is no spatial confounder as such (in the form of a missing or unmeasured spatial variable), but bias arises due to mis-specification of the covariate in the analysis model. However, since  $\beta \mathcal{S} \mathbf{x} = \beta \mathbf{x} - \beta(\mathbf{x} - \mathcal{S} \mathbf{x})$ , the true data generation process can be written in the form of (2) with  $\mathbf{z} = -\beta(\mathbf{x} - \mathcal{S} \mathbf{x})$ , and we can therefore use our framework to assess the bias in this case. From the expression for  $\mathbf{z}$  we see that “confounding” is at the higher frequencies  $\mathbf{x} - \mathcal{S} \mathbf{x}$  of the covariate, and the lower frequencies  $\mathcal{S} \mathbf{x}$  of the covariate are unconfounded. Thus, by Corollary 1, the bias is given by  $\frac{-\beta \sum_{i=k+1}^n (\xi_{sp,i}^x)^2 w_i}{\sum_{i=1}^n (\xi_{sp,i}^x)^2 w_i}$ . As the sample size  $n$  goes to infinity, we expect the higher frequencies to increasingly dominate  $\mathbf{x}$  and therefore the bias to approach  $-\beta$ , consistent with the results of Bolin and Wallin (2024).

### 5.3 Capped spatial+

Based on our analysis in Section 5.2, we present an adapted version of spatial+ which can be used to assess the bias in the more challenging Case 2 scenario. As previously noted, unconfounded high frequencies in  $\mathbf{x}$  have a similar effect on the bias as non-spatial information. Therefore, assuming the  $k$  highest

frequencies are unconfounded, a natural way to adapt spatial+ is the following two-step procedure. Let  $\mathbf{u}_{sp,1}, \dots, \mathbf{u}_{sp,n}$  denote the spatial eigenvectors in  $\mathbb{R}^n$ .

- (i) Decompose the covariate as  $\mathbf{x} = \mathbf{x}_{sp}^k + \mathbf{r}^k$  where  $\mathbf{x}_{sp}^k = \sum_{i=1}^{n-k} \xi_{sp,i}^x \mathbf{u}_{sp,i}$  (the lowest  $n-k$  frequencies) and  $\mathbf{r}^k = \sum_{i=n-k+1}^n \xi_{sp,i}^x \mathbf{u}_{sp,i}$  (the highest  $k$  frequencies).
- (ii) Estimate the covariate effect  $\beta$  by fitting the model (3) but with  $\mathbf{x}$  replaced by  $\mathbf{r}^k$ .

Proposition 1 shows that the bias of the corresponding covariate effect estimate is  $\langle \mathbf{r}^k, \mathbf{z} \rangle_{\Sigma^{-1}} / \langle \mathbf{r}^k, \mathbf{r}^k \rangle_{\Sigma^{-1}}$ , which, as  $\mathbf{r}^k$  is assumed to be unconfounded, should therefore, in theory, be 0. However, as the spatial eigenvectors span the whole of  $\mathbb{R}^n$ ,  $\mathbf{r}^k$  and  $\mathbf{z}$  no longer lie in orthogonal subspaces. As the component  $\mathbf{r}^k$  can also be modelled as part of the highest frequencies of the spatial effect in (3), the estimate of  $\beta$  obtained in this way is highly sensitive to inaccuracies at these frequencies of the estimated spatial effect. Such inaccuracies easily arise in practice as the estimation is based on overall spatial smoothing, driven by the fitted values rather than the behaviour at individual spatial frequencies. In order to avoid such sensitivity, we adapt the model matrix of the regression in (ii) by removing the columns corresponding to the frequencies above  $k$ . This more explicitly reflects the assumption of unconfoundedness at these frequencies but allows the spatial effect to continue to adjust for confounders at frequencies below the cap. We call the estimate of  $\beta$  obtained from (i) and the adapted (ii) the capped spatial+ estimate. By construction, if the assumption of unconfoundedness above the cap is true, the bias for this estimate is 0.

In practice, the true value of the cap  $k$  is unlikely to be known, and it may therefore be mis-specified at a value  $k' \neq k$ . If  $k' < k$ ,  $\mathbf{r}^{k'} = \sum_{i=n-k'+1}^n \xi_{sp,i}^x \mathbf{u}_{sp,i}$  is simply a smaller component of  $\mathbf{r}^k$  which is still orthogonal to the spatial part of the adjusted spatial model. Therefore, the bias should still be eliminated. However, if  $k' > k$ , then  $\mathbf{r}^{k'}$  contains a potentially confounded component of  $\mathbf{x}$ , namely, the  $k' - k$  highest frequencies of  $\mathbf{x}_{sp}^k$ , and by Corollary 1 the bias becomes  $\sum_{i=n-k'+1}^{n-k} \xi_{sp,i}^x \xi_{sp,i}^z w_i / \sum_{i=n-k'+1}^n (\xi_{sp,i}^x)^2 w_i$ . For comparison, the bias in the original spatial model (3) in this scenario is  $\sum_{i=1}^{n-k} \xi_{sp,i}^x \xi_{sp,i}^z w_i / \sum_{i=1}^n (\xi_{sp,i}^x)^2 w_i$ . Thus, the numerator for the spatial model includes additional confounded frequencies contributing to the bias, but at the same time the denominator is also larger. Therefore, in this case, the capped spatial+ estimate may not reduce and could even increase the size of the bias of the spatial model.

For a given data set in the Case 2 scenario of Section 5.2, under the assumption of unconfoundedness at the highest frequencies, the bias can therefore be assessed using capped spatial+ with a range of caps  $k'$ . Starting at small values of  $k'$ , the corresponding estimate of  $\beta$  should be unbiased and therefore stay stable as we increase  $k'$ , but when  $k'$  reaches the true cap  $k$ , the estimate changes due to the introduction of confounding bias. Thus, if we observe stable capped spatial+ estimates for caps below a certain value, these estimates can be expected to be unbiased.

Finally, in Section 5.2 we noted that the assumption of unconfoundedness does not have to be limited to the highest frequencies of the spatial effect. If we believe the unconfounded behaviour of  $\mathbf{x}$  is in a different frequency range, we can easily adapt the capped spatial+ method by replacing the component  $\mathbf{r}^k$  by the part of  $\mathbf{x}$  that is believed to be unconfounded. In the scenario of Bolin and Wallin (2024) described at the end of Section 5.2, we could use the  $k$  lowest frequencies of  $\mathbf{x}$  as the component  $\mathbf{r}^k$  under the assumption that these are contained in the unconfounded low frequency component  $\mathcal{S}\mathbf{x}$  of the covariate. This is therefore also consistent with the suggestion in Bolin and Wallin (2024) to replace  $\mathbf{x}$  in the analysis model (3) by a smoothed (i.e. lower frequency) version  $\hat{\mathcal{S}}\mathbf{x}$  of the covariate.

## 5.4 Simulations for capped spatial+

In this section, we use simulations to illustrate the ideas behind the capped spatial+ method proposed in Section 5.3. For a fixed value of the cap  $k$  we simulate data in which the covariate  $\mathbf{x}$  is fully spatial but the  $k$  highest frequencies are unconfounded. We then consider the bias in the spatial model (3) as well as the capped spatial+ estimates for different values of the cap.

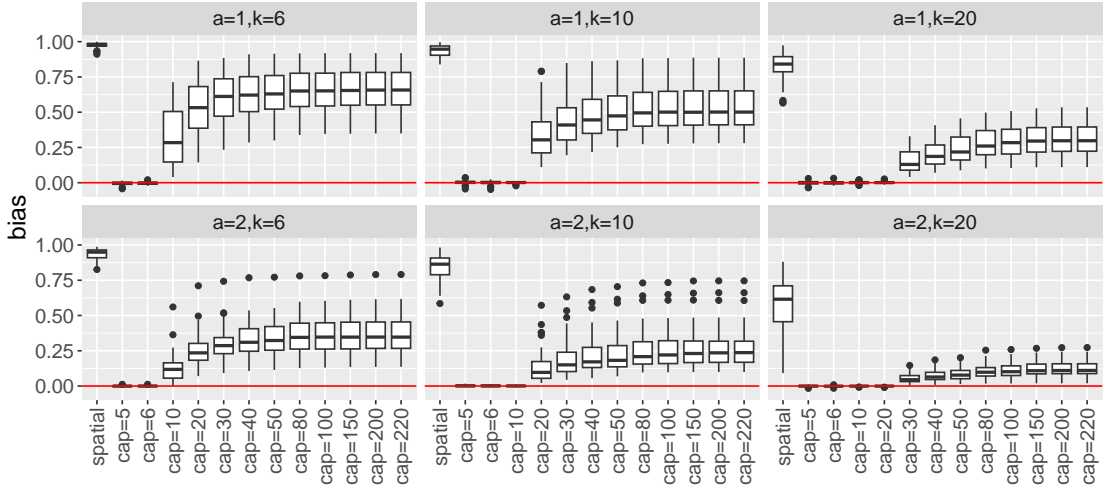


Figure 3: Bias of  $\hat{\beta}$  in the spatial and capped spatial+ models with different combinations of  $k \in \{5, 10, 20\}$  and  $a \in \{1, 2\}$ . The true value is  $\beta = 1$ . All other parameters remain constant.

The data is generated such that:

$$\mathbf{y} = \beta \mathbf{x} + \mathbf{z} + \epsilon^y, \quad \mathbf{x} = \mathbf{z}_{\text{sp,low}}^x + \mathbf{z}_{\text{sp,medium}}^x + a \mathbf{z}_{\text{sp,high}}^x, \quad \mathbf{z} = \mathbf{z}_{\text{sp,low}}^z + \mathbf{z}_{\text{sp,medium}}^z$$

where  $\epsilon^y \sim N(\mathbf{0}, \sigma^2 \mathbf{I})$  and  $a > 0$  controls the size of the unconfounded high frequency spatial component in  $\mathbf{x}$ . In order to generate  $\mathbf{z}_{\text{sp,low}}^x$ ,  $\mathbf{z}_{\text{sp,high}}^x$  and  $\mathbf{z}_{\text{sp,medium}}^x$ , we fit a thin plate spline to a realization of a Gaussian process with  $\kappa = 0.5/3$  (see beginning of the section), where the penalty and design matrix have now been reparameterised such that they only consider the 100 lowest, the  $k$  highest and all medium frequencies, respectively;  $\mathbf{z}_{\text{sp,low}}^z$  is generated similarly to Section 4 but it is fitted to a new realization of a Gaussian process with  $\kappa = 0.5/3$  using only the 100 lowest basis functions. We consider  $k \in \{5, 10, 20\}$  and  $a \in \{1, 2\}$  in the data generating process;  $\beta = 1$ ,  $\sigma = 0.1$ ,  $n = 1000$ ,  $N = 50$ . The reparametrisation is explained in Appendix 2.

In the data analysis model, the capped spatial+ model uses a reparameterised  $\tilde{\mathbf{B}}_{\text{sp}}$  and  $\tilde{\beta}_{\text{sp}}$  in the design and penalty matrix for the spatial effects in the first and second stage equation of spatial+ with  $\text{cap} \in \{5, 10, 15, 20, 25, 30, 40, 50\}$ , so that we consider cases where the used cap is above, below or equal to the true cap  $k$ . Unlike the standard spatial+, this allows us to control the frequencies included in the spatial effects for  $\mathbf{y}$  and  $\mathbf{x}$ , such that ideally  $\mathbf{r}^x$  should not have any confounded frequencies. Here, on the first stage regression for  $\mathbf{x}$  we use no smoothing in order to guarantee the residuals  $\mathbf{r}^x$  are orthogonal to the subspace spanned by  $\tilde{\mathbf{B}}_{\text{sp}} \tilde{\beta}_{\text{sp}}$ . We use  $n$  basis functions in the spatial model.

In Figure 3 we see that the bias decreases for increasing  $k$  and  $a$ . This is expected from our results as a larger  $k$  implies fewer confounded medium frequencies and more unconfounded high frequencies, while a larger  $a$  implies a larger proportion of unconfounded high frequencies in  $\mathbf{x}$ . For  $\text{cap} \leq k$ , we are able to completely remove confounding bias, even if only using a smaller fraction of the unconfounded high frequency component in  $\mathbf{x}$  to identify the effect. When the  $k < \text{cap}$  the residuals in spatial+ contain medium frequency confounding and, quite noticeably, bias arises. Thus, we observe a constant bias of zero for caps below  $k$  and a considerable increase for caps above  $k$ . The MSE for the predicted values reveals that in general capping increases MSE, although quite negligibly for  $k \leq \text{cap}$ , when compared to the drastic increase observed for  $k > \text{cap}$  (see Appendix 3.1).

## 6 Application to air temperature in Germany

As an empirical illustration, we analyse the relationship between the monthly mean temperature at two metres above ground, treated here as the response, and the monthly mean precipitation, the covariate, in Germany for the year 2010 at 336 locations. The data are open access and provided by the German Meteorological Service (DWD). For convenience, precipitation is measured in units of 10 millimetres and temperature is measured in degrees Celsius. In the context of spatial confounding, climate is a compelling example, as both covariates and response can exhibit relatively larger or narrower spatial correlation ranges, also depending on the time of year.

Independent regression models are fitted to each month, where rainfall and temperature are first standardised and the resulting regression coefficient for rainfall is converted back to the original scale. We consider regression models: (1) capped spatial+ (see Section 5.3), (2) spatial, (3) non-spatial. By comparing the results of (1) and (2), we show how capped spatial+ can help identify problematic covariate effect estimates in the spatial model and suggest appropriate adjustments.

All spatial effects are modelled with thin plate regression splines in `mgcv` (Wood, 2024). The results are shown in Figure 4. When the cap used for capped spatial+ is very small, estimates of the covariate effect may not be reliable, as the residuals will be very small and unlikely to have sufficient information about the covariate. On the other hand, as the cap increases, the fit of the model deteriorates. Therefore, we only show the estimates with  $cap = 5, 6, \dots, 15$  which are also statistically significant at the 95% confidence level. From September to January and May, the caps (below 15) are generally insignificant, as indicated by the lack of pink dots in the plot. In the other months, the capped spatial+ estimates can be used to assess whether we have confidence in the spatial estimate, and the dots show how the estimate should likely be adjusted. November is perhaps the most puzzling, where the coefficients appear to be either positive or negative depending on the frequencies included in capped spatial+. On closer inspection, this can be explained by a more complex spatial structure of precipitation in this month, with many localised patterns, so that a linear effect of precipitation may not be sufficient in general. With the exception of November and December, all estimates plotted in Figure 4 are negative, indicating a generally negative association between the two variables.

In order to understand the observed behaviour in more detail, we focus on three months: January, April and August. For these three months, results for caps up to 9, including the AIC and RMSE of the different models, are shown in Table 1. We start with the spring and summer months. In April, the capped spatial+ estimates are lower in absolute value than those of the spatial model. This may indicate that the spatial model estimate is biased, and under the assumption that the highest frequencies are unconfounded, the estimate should be adjusted down (in absolute terms). In August, the estimates for all models appear to be fairly consistent, with little variability in the capped spatial+ estimates. This suggests that unobserved spatial confounders are not affecting the estimation and the spatial model estimate does not need to be adjusted. In January, we know from Figure 4 that none of the capped spatial+ estimates up to a cap of 15 are statistically significant. This suggests that the highest frequencies (up to 15) in the spatial effect are not helping us to identify the effect of rainfall and may simply not be present in this particular covariate. As mentioned in Section 5.2, however, when a covariate is dominated by low frequencies, the estimate in the spatial model may well be biased. In this case, we can adapt the capped spatial+ method to identify the highest frequencies at which  $x$  has a significant effect. Assuming that these frequencies are unconfounded, we can use the corresponding capped spatial+ estimate to assess the bias. We use a sliding window technique that systematically removes 15 consecutive frequencies, starting progressively deeper into the low frequency spectrum, where  $start$  is the starting frequency. Figure 4 shows the estimates for the first two sliding windows, with significant estimates at the 5% level represented by triangles. We can see that in January the spatial model may overestimate the effect (in absolute terms). We followed the same approach for all the remaining autumn and winter months and for May. The results suggest that the extra peak building up to October may be an artefact, with values likely closer to flat around

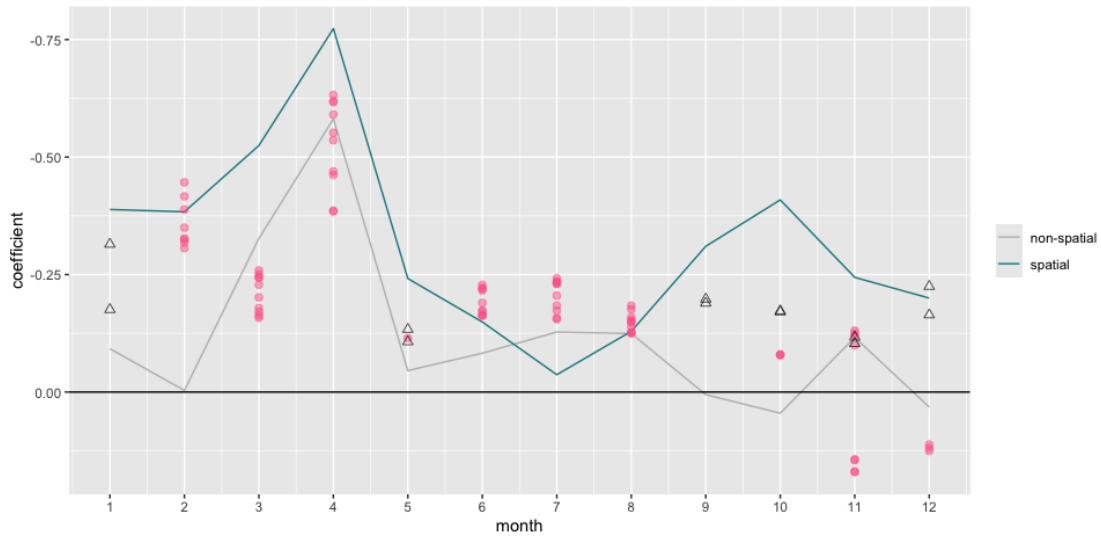


Figure 4: Coefficient estimates of  $\hat{\beta}$ . The solid lines correspond to the spatial model (teal), the non-spatial model (grey) and a coefficient estimate of zero (black). The pink dots show the statistically significant at 5% estimates of the capped spatial+ for the first 15 caps. The triangles show the first two statistically significant results from capped spatial+ using the sliding window.

–0.125. Apart from the peak in April – perhaps a case of “Der April macht, was er will” (“April does as it pleases”) – the coefficients remain relatively stable. In all the months analysed using the sliding window technique, the first significant coefficient appears the latest at  $start = 8$ , except in September, where it appears at  $start = 38$ .

## 7 Discussion

As illustrated in this paper, the analytical expressions derived in Proposition 1 and Corollary 1 provide an intuitive framework for explaining and, indeed, demystifying the bias arising from spatial confounding. In particular, we show that bias in the spatial model is caused by spatial smoothing and can become arbitrarily large. In practical applications, the difference between the estimates in the spatial and non-spatial models is commonly seen as an indicator of spatial confounding. However, our analysis and simulations show that a difference between these estimates does not in itself show whether the estimate in the spatial model is biased. Instead we propose using the methods set out in Section 5 to assess and adjust for the bias.

As most other work on spatial confounding, the focus in this paper has been on quantifying the bias in spatial regressions. A derivation and short discussion about the variance of the covariate effect estimate is included in Appendix 1.6. However, to put the bias into perspective and thoroughly conduct statistical inference, more investigations on associated uncertainty will be an important direction for future research.

## Data availability statement

The data is publicly available on the website of the German weather service (DWD). We provide code for all analyses in the paper, which includes instructions on how to download the data.

Table 1: Coefficient estimates for the regression models fitted to average monthly air temperature.

month	model/cap	$\hat{\beta}$	p-value	AIC	RMSE
1	non-spatial	-0.0922849	0.0524941	1306.6419	0.9897
1	spatial	-0.3885536	0.0000000	650.9834	0.1441
1	cap =5	-0.1847219	0.1679208	870.5588	0.2706
1	cap =6	0.0654211	0.5980586	893.6362	0.2911
1	cap =7	0.1690087	0.1617385	903.5738	0.3013
1	cap =8	0.1773077	0.1480378	915.2859	0.3124
1	cap =9	0.0240164	0.7846951	917.0572	0.3159
4	non-spatial	-0.5811757	0.0000000	1196.6612	0.7748
4	spatial	-0.7732586	0.0000000	951.3315	0.3053
4	cap = 5	-0.6189845	0.0000023	1095.9985	0.4349
4	cap = 6	-0.5906941	0.0000051	1096.8946	0.4380
4	cap = 7	-0.6318752	0.0000005	1098.1054	0.4404
4	cap = 8	-0.6166930	0.0000002	1096.3102	0.4387
4	cap = 9	-0.3856196	0.0013258	1148.0541	0.5282
8	non-spatial	-0.1244348	0.0000000	1231.8161	0.8173
8	spatial	-0.1292622	0.0000000	1012.2477	0.3297
8	cap =5	-0.1382547	0.0000314	1157.0444	0.5120
8	cap =6	-0.1262546	0.0000555	1156.6078	0.5134
8	cap =7	-0.1248357	0.0000148	1155.2212	0.5126
8	cap =8	-0.1270226	0.0000038	1153.4515	0.5106
8	cap =9	-0.1530327	0.0000000	1154.1968	0.5184

## References

Adin, A., Goicoa, T., Hodges, J. S., Schnell, P. M., and Ugarte, M. D. (2023). Alleviating confounding in spatio-temporal areal models with an application on crimes against women in india. *Statistical Modelling*, 23(1):9–30.

Bobb, J. F., Cruz, M. F., Mooney, S. J., Drewnowski, A., Arterburn, D., and Cook, A. J. (2022). Accounting for spatial confounding in epidemiological studies with individual-level exposures: An exposure-penalized spline approach. *Journal of the Royal Statistical Society Series A: Statistics in Society*, 185(3):1271–1293.

Bolin, D. and Wallin, J. (2024). Spatial confounding under infill asymptotics. *arXiv preprint arXiv:2403.18961*.

Bradley, J. R. (2024). Spatial deconfounding is reasonable statistical practice: Interpretations, clarifications, and new benefits. *arXiv preprint arXiv:2408.05106*.

Briz-Redón, Á. (2023). On alleviating spatial confounding issues with the Bayesian Lasso. *Research Square preprint, doi:10.21203/rs.3.rs-2498913/v1*.

Clayton, D. G., Bernardinelli, L., and Montomoli, C. (1993). Spatial correlation in ecological analysis. *International Journal of Epidemiology*, 22(6):1193–1202.

Dupont, E., Wood, S. N., and Augustin, N. (2022). Spatial+: A novel approach to spatial confounding. *Biometrics*, 78(4):1279–1290.

Fahrmeir, L. and Kneib, T. (2011). *Bayesian Smoothing and Regression for Longitudinal, Spatial and Event History Data*. Oxford University Press.

Gilbert, B., Ogburn, E. L., and Datta, A. (2024). Consistency of common spatial estimators under spatial confounding. *Biometrika*, page asae070.

Guan, Y., Page, G. L., Reich, B. J., Ventrucci, M., and Yang, S. (2023). Spectral adjustment for spatial confounding. *Biometrika*, 110(3):699—719.

Hanks, E. M., Schliep, E. M., Hooten, M. B., and Hoeting, J. A. (2015). Restricted spatial regression in practice: geostatistical models, confounding, and robustness under model misspecification. *Environmetrics*, 26(4):243–254.

Hefley, T. J., Hooten, M. B., Hanks, E. M., Russell, R. E., and Walsh, D. P. (2017). The bayesian group lasso for confounded spatial data. *Journal of Agricultural, Biological and Environmental Statistics*, 22(1):42–59.

Hodges, J. S. and Reich, B. J. (2010). Adding spatially-correlated errors can mess up the fixed effect you love. *The American Statistician*, 64(4):325–334.

Hughes, J. and Haran, M. (2013). Dimension reduction and alleviation of confounding for spatial generalized linear mixed models. *Journal of the Royal Statistical Society: Series B (Statistical Methodology)*, 75(1):139–159.

Keller, J. P. and Szpiro, A. A. (2020). Selecting a scale for spatial confounding adjustment. *Journal of the Royal Statistical Society Series A: Statistics in Society*, 183(3):1121–1143.

Khan, K. and Berrett, C. (2023). Re-thinking spatial confounding in spatial linear mixed models. *arXiv preprint arXiv:2301.05743*.

Khan, K. and Calder, C. A. (2022). Restricted spatial regression methods: implications for inference. *Journal of the American Statistical Association*, 117(537):482–494.

Marques, I., Kneib, T., and Klein, N. (2022). Mitigating spatial confounding by explicitly correlating gaussian random fields. *Environmetrics*, 33(5):e2727.

Nobre, W. S., Schmidt, A. M., and Pereira, J. B. M. (2021). On the effects of spatial confounding in hierarchical models. *International Statistical Review*, 89(2):302–322.

Paciorek, C. J. (2010). The importance of scale for spatial-confounding bias and precision of spatial regression estimators. *Statistical Science*, 25(1):107–125.

Page, G. L., Liu, Y., He, Z., and Sun, D. (2017). Estimation and prediction in the presence of spatial confounding for spatial linear models. *Scandinavian Journal of Statistics*, 44(3):780–797.

Papadogeorgou, G., Choirat, C., and Zigler, C. M. (2019). Adjusting for unmeasured spatial confounding with distance adjusted propensity score matching. *Biostatistics*, 20(2):256–272.

Reich, B. J., Hodges, J. S., and Zadnik, V. (2006). Effects of residual smoothing on the posterior of the fixed effects in disease-mapping models. *Biometrics*, 62(4):1197–1206.

Reich, B. J., Yang, S., Guan, Y., Giffin, A. B., Miller, M. J., and Rappold, A. G. (2021). A review of spatial causal inference methods for environmental and epidemiological applications. *International Statistical Review*, 89(3):605–634.

Schnell, P. M. and Bose, M. (2019). Spectral parameterization for linear mixed models applied to confounding of fixed effects by random effects. *Journal of Statistical Planning and Inference*, 200:47–62.

Schnell, P. M. and Papadogeorgou, G. (2020). Mitigating unobserved spatial confounding when estimating the effect of supermarket access on cardiovascular disease deaths. *The Annals of Applied Statistics*, 14(4):2069–2095.

Thaden, H. and Kneib, T. (2018). Structural equation models for dealing with spatial confounding. *The American Statistician*, 72(3):239–252.

Urdangarin Iztueta, A., Goicoa Mangado, T., and Ugarte Martínez, M. D. (2022). Evaluating recent methods to overcome spatial confounding. *Revista Matemática Complutense* 1-28.

Wood, S. N. (2003). Thin plate regression splines. *Journal of the Royal Statistical Society Series B: Statistical Methodology*, 65(1):95–114.

Wood, S. N. (2024). *mgcv: Mixed GAM Computation Vehicle with Automatic Smoothness Estimation*. R package version 1.9-1.

Zimmerman, D. L. and Ver Hoef, J. M. (2022). On deconfounding spatial confounding in linear models. *The American Statistician*, 76(2):159–167.

# Supporting Information for “Demystifying Spatial Confounding” by E. Dupont, I. Marques and T. Kneib

July 1, 2025

## Abstract

In this appendix, we provide proofs as well as additional analysis and simulation results, supporting the material in the main paper.

## 1 Proofs and theoretical results

### 1.1 The spatial precision matrix $\Sigma^{-1}$

Central to our analyses are the properties of the precision matrix  $\Sigma^{-1}$ , in particular, its eigenvalues, which are computed in Lemma 1. First we have the following preliminary results.

**Lemma A.1.** *The inverse of the covariance structure  $\Sigma$  is given by  $\Sigma^{-1} = \sigma^{-2}(\mathbf{I} - \mathbf{A})$ , where  $\mathbf{A} = \sigma^{-2}\mathbf{B}_{\text{sp}}(\sigma^{-2}\mathbf{B}_{\text{sp}}^T\mathbf{B}_{\text{sp}} + \lambda\mathbf{S})^{-1}\mathbf{B}_{\text{sp}}^T$  is the influence matrix of a purely spatial model, i.e. a model only containing the spatial effect.*

*Proof.* Let  $\mathbf{M} = \sigma^{-2}(\mathbf{I} - \mathbf{A})$ . Then

$$\begin{aligned}\Sigma\mathbf{M} &= (\sigma^2\mathbf{I} + \lambda^{-1}\mathbf{B}_{\text{sp}}\mathbf{S}^{-1}\mathbf{B}_{\text{sp}}^T)(\sigma^{-2}\mathbf{I} - \sigma^{-4}\mathbf{B}_{\text{sp}}(\sigma^{-2}\mathbf{B}_{\text{sp}}^T\mathbf{B}_{\text{sp}} + \lambda\mathbf{S})^{-1}\mathbf{B}_{\text{sp}}^T) \\ &= \mathbf{I} + \sigma^{-2}\lambda^{-1}\mathbf{B}_{\text{sp}}\mathbf{S}^{-1}\mathbf{B}_{\text{sp}}^T - \sigma^{-2}\mathbf{B}_{\text{sp}}(\sigma^{-2}\mathbf{B}_{\text{sp}}^T\mathbf{B}_{\text{sp}} + \lambda\mathbf{S})^{-1}\mathbf{B}_{\text{sp}}^T \\ &\quad - \sigma^{-4}\lambda^{-1}\mathbf{B}_{\text{sp}}\mathbf{S}^{-1}\mathbf{B}_{\text{sp}}^T\mathbf{B}_{\text{sp}}(\sigma^{-2}\mathbf{B}_{\text{sp}}^T\mathbf{B}_{\text{sp}} + \lambda\mathbf{S})^{-1}\mathbf{B}_{\text{sp}}^T \\ &= \mathbf{I} + \sigma^{-2}\lambda^{-1}\mathbf{B}_{\text{sp}}\mathbf{S}^{-1}(\mathbf{I} - (\lambda\mathbf{S} + \sigma^{-2}\mathbf{B}_{\text{sp}}^T\mathbf{B}_{\text{sp}})(\sigma^{-2}\mathbf{B}_{\text{sp}}^T\mathbf{B}_{\text{sp}} + \lambda\mathbf{S})^{-1})\mathbf{B}_{\text{sp}}^T \\ &= \mathbf{I}.\end{aligned}$$

Hence  $\Sigma^{-1} = \mathbf{M}$ . □

**Lemma A.2.** *Let  $\alpha_1 \leq \dots \leq \alpha_p$  be the eigenvalues of the penalty matrix  $\mathbf{S}$  and  $\lambda > 0$  the smoothing parameter. Then the influence matrix  $\mathbf{A} = \sigma^{-2}\mathbf{B}_{\text{sp}}(\sigma^{-2}\mathbf{B}_{\text{sp}}^T\mathbf{B}_{\text{sp}} + \lambda\mathbf{S})^{-1}\mathbf{B}_{\text{sp}}^T$  is symmetric positive semi-definite and its eigenvalues are given by  $\{0, \alpha'_1, \dots, \alpha'_p\}$  where  $\alpha'_i = \sigma^{-2}/(\sigma^{-2} + \lambda\alpha_i)$  for  $i = 1, \dots, p$ .*

*Proof.* As  $\mathbf{S}$  is symmetric,  $\mathbf{A}$  is also symmetric. Without loss of generality we can assume that the spatial basis  $\mathbf{B}_{\text{sp}}$  is orthonormal so that  $\mathbf{B}_{\text{sp}}^T \mathbf{B}_{\text{sp}} = \mathbf{I}$  and

$$\mathbf{A} = \sigma^{-2} \mathbf{B}_{\text{sp}} (\sigma^{-2} \mathbf{I} + \lambda \mathbf{S})^{-1} \mathbf{B}_{\text{sp}}^T.$$

Clearly anything in the null space of  $\mathbf{A}$  (i.e. the orthogonal complement of the column space of  $\mathbf{B}_{\text{sp}}$ , which is the “non-spatial” part of  $\mathbb{R}^n$ ) is an eigenvector with eigenvalue 0.

Suppose  $\mathbf{v} \in \mathbb{R}^p$  is an eigenvector of  $\mathbf{S}$  with eigenvalue  $\alpha_i$ . Let  $\mathbf{v}' = \mathbf{B}_{\text{sp}} \mathbf{v}$ . Then  $\mathbf{v}' \in \mathbb{R}^n$  and

$$\begin{aligned} \mathbf{A} \mathbf{v}' &= \sigma^{-2} \mathbf{B}_{\text{sp}} (\sigma^{-2} \mathbf{I} + \lambda \mathbf{S})^{-1} \mathbf{B}_{\text{sp}}^T \mathbf{B}_{\text{sp}} \mathbf{v}' \\ &= \sigma^{-2} \mathbf{B}_{\text{sp}} (\sigma^{-2} \mathbf{I} + \lambda \mathbf{S})^{-1} \mathbf{v}' \\ &= \sigma^{-2} \mathbf{B}_{\text{sp}} (\sigma^{-2} + \lambda \alpha_i)^{-1} \mathbf{v}' \\ &= \frac{\sigma^{-2}}{\sigma^{-2} + \lambda \alpha_i} \mathbf{v}'. \end{aligned}$$

Since all eigenvalues are non-negative,  $\mathbf{A}$  is positive semi-definite.  $\square$

Lemma A.2 gives some insight into the mechanism of smoothing within the spatial data analysis model (3). Since  $\mathbf{A}$  is the influence matrix of a purely spatial model, the estimated spatial effect in model (3) is given by  $\hat{\mathbf{z}} = \mathbf{B}_{\text{sp}} \hat{\beta}_{\text{sp}} = \mathbf{A}(\mathbf{y} - \hat{\beta} \mathbf{x})$ . So each eigenvalue of  $\mathbf{A}$  tells us how much weight the corresponding eigenvector is given within the estimated spatial effect. The “non-spatial” part of  $\mathbb{R}^n$  is spanned by eigenvectors with eigenvalue 0 and therefore contributes nothing to the estimated spatial effect. The remaining eigenvalues  $\alpha'_1, \dots, \alpha'_p$  satisfy  $0 < \alpha'_p \leq \dots \leq \alpha'_1 \leq 1$  with  $\alpha'_i = 1$  if and only if  $\lambda \alpha_i = 0$ . Since  $\lambda > 0$ , only unpenalised spatial basis vectors (i.e. eigenvectors with  $\alpha_i = 0$ ) are given the maximum weight of 1 in the estimated spatial effect. For all other spatial basis vectors, smoothing reduces the weight of the contribution to less than 1, and the larger the value of  $\alpha_i$  (i.e. the higher the penalisation) the smaller the contribution of the corresponding eigenvector. As higher frequency eigenvectors are typically those with the highest penalisation, these contribute least to the estimated spatial effect in line with intuition.

The smoothing parameter  $\lambda$  controls the overall level of smoothing with larger values of  $\lambda$  (i.e. more smoothing) leading to a smaller contribution of all spatial basis vectors to the estimated effect. At the other extreme ( $\lambda \rightarrow 0$ ) is an entirely unsmoothed spatial effect which gives the maximum weight of 1 to all eigenvectors.

Combining Lemmas A.1 and A.2 we can now prove Lemma 1:

*Proof of Lemma 1.* By Lemma A.1 we have that  $\Sigma^{-1} = \sigma^{-2}(\mathbf{I} - \mathbf{A})$  so the eigenvalues of  $\Sigma^{-1}$  are all of the form  $\sigma^{-2}(1 - \alpha)$  where  $\alpha$  is an eigenvalue of  $\mathbf{A}$ . Lemma A.2 gives us the eigenvalues of  $\mathbf{A}$ . The eigenvalue  $\alpha = 0$  (corresponding to the eigenvectors spanning the non-spatial part of  $\mathbb{R}^n$ ) leads to the eigenvalue  $\sigma^{-2}$  for  $\Sigma^{-1}$  and the remaining eigenvalues of  $\Sigma^{-1}$  are given by

$$\sigma^{-2}(1 - \frac{\sigma^{-2}}{\sigma^{-2} + \lambda \alpha_i}) = \frac{\sigma^{-2} \lambda \alpha_i}{\sigma^{-2} + \lambda \alpha_i}, \quad \text{for } i = 1, \dots, p.$$

$\square$

## 1.2 Spatial frequencies

Although the spatial confounding literature often emphasises the importance of spatial frequencies, there is no single definition of what spatial frequencies are. In the seminal work of Paciorek (2010), and later Page et al. (2017), who considered the impact of spatial scales on spatial confounding in Gaussian process models, spatial scale was defined through the model parameters. More recent work such as Guan et al. (2023) and Keller and Szpiro (2020) use spectral frequencies, i.e. spatial Fourier expansions. Keller and Szpiro (2020) also suggest analysing spatial behaviour using wavelets. While Fourier and wavelet analyses are well-established exploratory tools for investigating frequency behaviours, they have some disadvantages, e.g. Fourier analysis assumes spatial stationarity (which may be unrealistic in practice), and wavelet analysis requires subjective choices around the type of wavelet basis, the smoothness of basis functions etc. For discrete spatial models the notion of spatial frequencies is perhaps even harder to define, but e.g. for the ICAR random effects model with one data point per region, Guan et al. (2023) use eigenvectors related to the spatial precision matrix of the model.

In this paper, irrespective of whether the spatial analysis model is discrete or continuous and the choice of the spatial effect, we use the eigenvectors of the precision matrix  $\Sigma^{-1}$  to represent different spatial frequencies. Here we show in more detail how these eigenvectors form a natural representation of spatial frequencies. Firstly, for all spatial models, the underlying assumption is that nearby observations are more similar than observations far apart. Therefore, irrespective of the exact specification of the spatial random effect, the resulting smoothing penalty  $\mathbf{S}$  is designed to penalise abrupt local changes (interpretable as high frequency spatial behaviour) more than changes that occur over larger distances (interpretable as low frequency behaviour). In other words, the penalty structure encodes, in a quantifiable way, what the model perceives as high versus low frequency spatial behaviour.

For a given choice of spatial analysis model, we now consider the  $n$  eigenvectors of the precision matrix  $\Sigma^{-1}$ . Each eigenvector represents a particular behaviour over space, and Lemma 1 shows that the size of the corresponding eigenvalue is directly linked to how much that behaviour is penalised. More specifically, there are  $n - p$  eigenvectors with eigenvalue  $\sigma^{-2}$ , i.e. these behaviours are unaffected by penalisation and can therefore be considered to be “non-spatial”, and for the remaining  $p$  eigenvectors, the eigenvalues are given by

$$\sigma^{-2}w_i, \quad w_i = \lambda\alpha_i/(\sigma^{-2} + \lambda\alpha_i)$$

with  $\alpha_1 \leq \dots \leq \alpha_p$  the eigenvalues of the penalty matrix  $\mathbf{S}$ . Although these  $p$  eigenvalues depend on the parameters  $\sigma^{-2}$  and  $\lambda$  (which are usually estimated), their ordering is the same as the  $\alpha_i$ ’s, i.e.  $\sigma^{-2}w_1 \leq \dots \leq \sigma^{-2}w_p$ . Thus, irrespective of the estimates of the parameters, a large/small eigenvalue corresponds exactly to high/low penalisation. Therefore, if we order the  $p$  spatial eigenvectors in ascending order of eigenvalues, the lowest spatial frequencies will be first and the highest spatial frequencies last. We illustrate this here using two examples (one discrete and one continuous).

### Example 1: Slovenia municipalities (discrete space model)

In this example we consider an ICAR random effects model with one observation in each region using the  $n = 212$  municipalities of Slovenia. In this case, the spatial random effect has dimension  $p = n$  so we can use the orthonormal spatial basis  $\mathbf{B}_{sp} = \mathbf{I}$  (as the spatial basis simply spans the whole space). The penalty matrix  $\mathbf{S}$  is the graph Laplacian of the neighbourhood structure defined by the map in Figure 1 (left). The spatial precision matrix is given by  $\Sigma^{-1} = \sigma^{-2}(\mathbf{I} - \mathbf{A})$  where  $\mathbf{A} = \sigma^{-2}(\sigma^{-2}\mathbf{I} + \lambda\mathbf{S})^{-1}$ . The  $n$  eigenvectors of  $\Sigma^{-1}$  are therefore equal to the  $p = n$  eigenvectors of  $\mathbf{S}$  and there are no non-spatial eigenvectors.

The eigenvalues  $\alpha_1 \leq \dots \leq \alpha_n$  of  $\mathbf{S}$  in ascending order are shown in Figure 1 (right). The eigenvalues of  $\Sigma^{-1}$  are given by  $\sigma^{-2}w_1 \leq \dots \leq \sigma^{-2}w_n$  where  $w_i = \lambda\alpha_i/(\sigma^{-2} + \lambda\alpha_i)$ . Figure 2 shows plots of four different eigenvectors in ascending order of eigenvalues. As expected, low/high eigenvalues result in low/high spatial frequency behaviours.

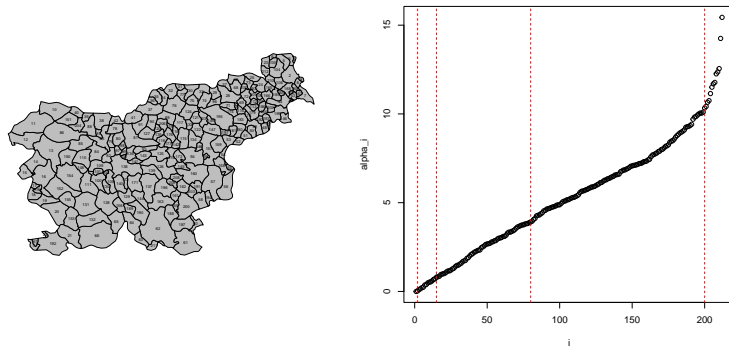


Figure 1: Slovenia example: Municipalities (left) and eigenvalues of  $\mathbf{S}$  in ascending order with vertical red lines showing the four ( $i = 2, 15, 80, 200$ ) used for the plots in Figure 2 (right).

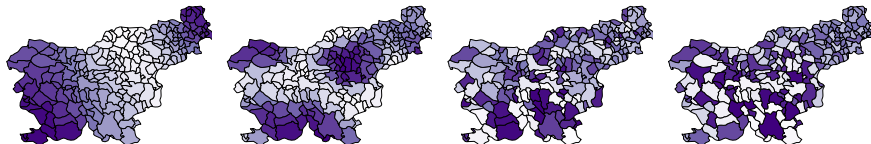


Figure 2: Slovenia example: Four spatial eigenvectors ( $i = 2, 15, 80, 200$ ) of  $\Sigma^{-1}$  in ascending order of eigenvalues from left to right.

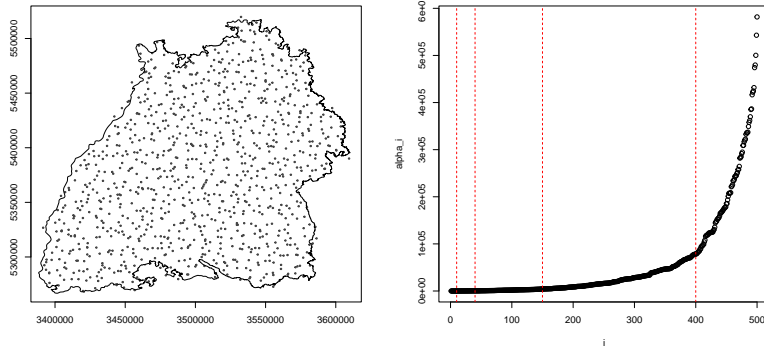


Figure 3: Baden-Württemberg example: Data locations (left) and eigenvalues of  $\mathbf{S}$  in ascending order with vertical red lines showing the four ( $i = 10, 40, 150, 400$ ) used for the plots in Figure 4

### Example 2: Baden-Württemberg (continuous space model)

In this example we have sampled  $n = 1000$  random locations across Baden-Württemberg, Germany (shown in Figure 3 (left)). We consider a thin plate regression spline model with  $k = 500$  basis functions for the spatial effect. So  $p = k < n$  and the model matrix for the spatial effect is the  $n \times k$  matrix where each column is a thin plate spline basis function evaluated at the data locations (including a constant column of 1's that represents the intercept). We define  $\mathbf{B}_{\text{sp}}$  to be the orthogonalised version of this model matrix (using Gram-Schmidt orthogonalisation). The matrix  $\mathbf{S}$  is the  $k \times k$  thin plate spline smoothing penalty (where the intercept has penalty 0) and the spatial precision matrix is the  $n \times n$  matrix given by  $\Sigma^{-1} = \sigma^{-2}(\mathbf{I} - \mathbf{A})$  where  $\mathbf{A} = \sigma^{-2}\mathbf{B}_{\text{sp}}(\sigma^{-2}\mathbf{I} + \lambda\mathbf{S})^{-1}\mathbf{B}_{\text{sp}}^T$ .

The proof of Lemma A.1 shows that if  $\mathbf{v}_1, \dots, \mathbf{v}_k$  are the ( $k$ -dimensional) eigenvectors of  $\mathbf{S}$  with eigenvalues  $\alpha_1 \leq \dots \leq \alpha_k$ , then  $\mathbf{v}'_i = \mathbf{B}_{\text{sp}}\mathbf{v}_i$ ,  $i = 1, \dots, k$ , are the ( $n$ -dimensional) spatial eigenvectors of  $\Sigma^{-1}$  with eigenvalues  $\sigma^{-2}w_1 \leq \dots \leq \sigma^{-2}w_k$ ,  $w_i = \lambda\alpha_i/(\sigma^{-2} + \lambda\alpha_i)$ . The remaining  $n - k$  eigenvectors of  $\Sigma^{-1}$  have eigenvalue  $\sigma^{-2}$  and span the “non-spatial” part of the sample space. So we see that the eigen-decomposition of  $\Sigma^{-1}$  somehow “translates” the smoothing that is specified in the smaller  $k$ -dimensional space into the  $n$ -dimensional sample space and gives a natural decomposition of the sample space into different spatial behaviours.

Figure 3 (right) shows the eigenvalues of  $\mathbf{S}$  in ascending order. Figure 4 shows plots of four different spatial eigenvectors in ascending order of eigenvalues. As the eigenvectors are only defined at the data locations, we have also shown spatially interpolated versions of these (using thin plate regression splines with basis size 900 for the interpolations). Once again, the plots confirm that low/high eigenvalues result in low/high spatial frequency behaviours.

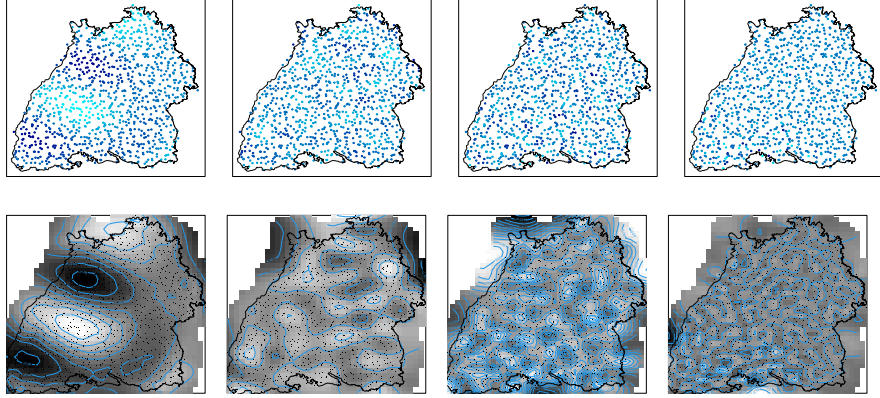


Figure 4: Baden-Württemberg example: Four eigenvectors ( $i = 10, 40, 150, 400$ ) of  $\Sigma^{-1}$  in ascending order of eigenvalues from left to right (top). Smooth interpolations of the same four eigenvectors (bottom).

### 1.3 Proof of Proposition 1

*Proof.* Since under the data generating model (2)  $E(\mathbf{y}) = \beta\mathbf{x} + \mathbf{z}$ , we have that

$$\begin{aligned}
 E(\hat{\beta}) &= (\mathbf{x}^T \Sigma^{-1} \mathbf{x})^{-1} \mathbf{x}^T \Sigma^{-1} E(\mathbf{y}) \\
 &= (\mathbf{x}^T \Sigma^{-1} \mathbf{x})^{-1} \mathbf{x}^T \Sigma^{-1} (\beta\mathbf{x} + \mathbf{z}) \\
 &= \beta + (\mathbf{x}^T \Sigma^{-1} \mathbf{x})^{-1} \mathbf{x}^T \Sigma^{-1} \mathbf{z} \\
 &= \beta + \frac{\langle \mathbf{x}, \mathbf{z} \rangle_{\Sigma^{-1}}}{\langle \mathbf{x}, \mathbf{x} \rangle_{\Sigma^{-1}}}.
 \end{aligned}$$

□

## 1.4 Proof of Corollary 1

*Proof.* The numerator of the bias in  $\hat{\beta}$  is given by

$$\begin{aligned}
\langle \mathbf{x}, \mathbf{z} \rangle_{\Sigma^{-1}} &= \mathbf{x}^T \Sigma^{-1} \mathbf{z} \\
&= \boldsymbol{\xi}^{xT} \mathbf{U}^T \Sigma^{-1} \mathbf{U} \boldsymbol{\xi}^z \\
&= \sigma^{-2} \boldsymbol{\xi}_{\text{ns}}^{xT} \boldsymbol{\xi}_{\text{ns}}^z + \sigma^{-2} \boldsymbol{\xi}_{\text{sp}}^{xT} \begin{bmatrix} w_1 & & \\ & \ddots & \\ & & w_p \end{bmatrix} \boldsymbol{\xi}_{\text{sp}}^z \\
&= \sigma^{-2} \boldsymbol{\xi}_{\text{sp}}^{xT} \begin{bmatrix} w_1 & & \\ & \ddots & \\ & & w_p \end{bmatrix} \boldsymbol{\xi}_{\text{sp}}^z \\
&= \sigma^{-2} \sum_{i=1}^p \xi_{\text{sp},i}^x \xi_{\text{sp},i}^z w_i.
\end{aligned}$$

Similarly, the denominator of the bias is given by

$$\begin{aligned}
\langle \mathbf{x}, \mathbf{x} \rangle_{\Sigma^{-1}} &= \sigma^{-2} \boldsymbol{\xi}_{\text{ns}}^{xT} \boldsymbol{\xi}_{\text{ns}}^x + \sigma^{-2} \boldsymbol{\xi}_{\text{sp}}^{xT} \begin{bmatrix} w_1 & & \\ & \ddots & \\ & & w_p \end{bmatrix} \boldsymbol{\xi}_{\text{sp}}^x \\
&= \sigma^{-2} \sum_{i=1}^{n-p} (\xi_{\text{ns},i}^x)^2 + \sigma^{-2} \sum_{i=1}^p (\xi_{\text{sp},i}^x)^2 w_i.
\end{aligned}$$

□

## 1.5 Comparison to the non-spatial model

Using the expressions in Corollaries 1 and 2, we compute the difference between the bias  $\text{Bias}_{\text{ns}} = E(\hat{\beta}_{\text{ns}}) - \beta$  in the non-spatial model (4) and the bias  $\text{Bias} = E(\hat{\beta}) - \beta$  in the spatial model (3). As we are mainly interested in comparing the size of the bias, for simplicity assume that all  $\xi_{\text{sp},i}^x \xi_{\text{sp},i}^z$  are positive. To simplify notation, let

$$C_{\text{ns}} = \sum_{i=1}^{n-p} (\xi_{\text{ns},i}^x)^2 \geq 0.$$

Then,

$$\begin{aligned}
\text{Bias}_{\text{ns}} - \text{Bias} &= \frac{\sum_{i=1}^p \xi_{\text{sp},i}^x \xi_{\text{sp},i}^z}{C_{\text{ns}} + \sum_{i=1}^p (\xi_{\text{sp},i}^x)^2} - \frac{\sum_{i=1}^p \xi_{\text{sp},i}^x \xi_{\text{sp},i}^z w_i}{C_{\text{ns}} + \sum_{i=1}^p (\xi_{\text{sp},i}^x)^2 w_i} \\
&= \frac{(\sum_{i=1}^p \xi_{\text{sp},i}^x \xi_{\text{sp},i}^z) (C_{\text{ns}} + \sum_{i=1}^p (\xi_{\text{sp},i}^x)^2 w_i)}{(C_{\text{ns}} + \sum_{i=1}^p (\xi_{\text{sp},i}^x)^2) (C_{\text{ns}} + \sum_{i=1}^p (\xi_{\text{sp},i}^x)^2 w_i)} \\
&\quad - \frac{(\sum_{i=1}^p \xi_{\text{sp},i}^x \xi_{\text{sp},i}^z w_i) (C_{\text{ns}} + \sum_{i=1}^p (\xi_{\text{sp},i}^x)^2)}{(C_{\text{ns}} + \sum_{i=1}^p (\xi_{\text{sp},i}^x)^2) (C_{\text{ns}} + \sum_{i=1}^p (\xi_{\text{sp},i}^x)^2 w_i)}.
\end{aligned}$$

The denominator of this expression is positive and the numerator can be written as

$$C_{\text{ns}} \sum_{i=1}^p \xi_{\text{sp},i}^x \xi_{\text{sp},i}^z (1 - w_i) + \sum_{i,j} \xi_{\text{sp},i}^x \xi_{\text{sp},i}^z (\xi_{\text{sp},j}^x)^2 (w_j - w_i).$$

Recall that  $0 \leq w_1 \leq \dots \leq w_p < 1$  and note that  $\xi_{\text{sp},i}^x \xi_{\text{sp},i}^z$  is non-zero exactly when frequency  $i$  is confounded. Therefore, the first term in the numerator is strictly positive whenever there is confounding and  $\mathbf{x}$  has non-spatial information, and is larger when confounded frequencies in  $\mathbf{x}$  have low weights (i.e. are the low frequencies). The second term can be written as

$$\sum_{i < j} (\xi_{\text{sp},i}^x \xi_{\text{sp},i}^z (\xi_{\text{sp},j}^x)^2 - \xi_{\text{sp},j}^x \xi_{\text{sp},j}^z (\xi_{\text{sp},i}^x)^2) (w_j - w_i).$$

Since  $w_j - w_i \geq 0$  for  $i < j$ , this shows that confounding at low frequencies ( $\xi_{\text{sp},i}^x \xi_{\text{sp},i}^z \neq 0$ ) contribute positively to the sum, whereas confounding at high frequencies ( $\xi_{\text{sp},j}^x \xi_{\text{sp},j}^z \neq 0$ ) contribute negatively. Conversely, unconfounded high frequencies ( $\xi_{\text{sp},j}^x \neq 0, \xi_{\text{sp},j}^z = 0$ ) contribute positively, while unconfounded low frequencies ( $\xi_{\text{sp},i}^x \neq 0, \xi_{\text{sp},i}^z = 0$ ) contribute negatively. Note that for a fixed unconfounded high frequency  $j$  the contribution is given by

$$(\xi_{\text{sp},j}^x)^2 \sum_{i=1}^{j-1} \xi_{\text{sp},i}^x \xi_{\text{sp},i}^z (w_j - w_i)$$

with weight  $w_j$  close to 1. This shows that unconfounded high frequencies enter the expression in a similar way to non-spatial information.

Therefore, when  $\mathbf{x}$  has sufficient non-spatial information or unconfounded high frequencies, then we can generally expect the bias of the non-spatial model to be higher than that of the spatial model, with the difference between the biases larger when there is a lot of confounding at low frequencies. However, the relationship between the two biases is subtle and, when confounding is at high frequencies, the bias in the spatial model could well exceed that of the non-spatial model.

## 1.6 Dependence on the smoothing parameter

We consider here how the expression for the bias given in Corollary 1 depends on the overall level of smoothing controlled by the smoothing parameter  $\lambda > 0$ . For each  $i = 1, \dots, p$ , consider the  $i$ 'th weight  $w_i$  as a function of  $\lambda$ :

$$w_i(\lambda) = \frac{\lambda \alpha_i}{\sigma^{-2} + \lambda \alpha_i}.$$

We see that  $\lim_{\lambda \rightarrow 0} w_i(\lambda) = 0$  and (unless  $\alpha_i = 0$  in which case  $w_i(\lambda) \equiv 0$  is constant)  $\lim_{\lambda \rightarrow \infty} w_i(\lambda) = 1$ . We also have that

$$w_i'(\lambda) = \frac{\alpha_i \sigma^{-2}}{(\sigma^{-2} + \lambda \alpha_i)^2} \geq 0.$$

Hence, the weights are either constant (and equal to 0) or increasing between 0 and 1.

Let

$$f(\lambda) = \frac{\sum_{i=1}^p \xi_{\text{sp},i}^x \xi_{\text{sp},i}^z w_i(\lambda)}{\sum_{i=1}^{n-p} (\xi_{\text{ns},i}^x)^2 + \sum_{i=1}^p (\xi_{\text{sp},i}^x)^2 w_i(\lambda)}$$

denote the bias in the spatial model for a given  $\mathbf{x}$  and  $\mathbf{z}$  as a function of  $\lambda$ . We then have that

$$\begin{aligned} f'(\lambda) &= \frac{(\sum_{i=1}^p \xi_{\text{sp},i}^x \xi_{\text{sp},i}^z w'_i(\lambda)) \left( \sum_{i=1}^{n-p} (\xi_{\text{ns},i}^x)^2 + \sum_{i=1}^p (\xi_{\text{sp},i}^x)^2 w_i(\lambda) \right)}{\left( \sum_{i=1}^{n-p} (\xi_{\text{ns},i}^x)^2 + \sum_{i=1}^p (\xi_{\text{sp},i}^x)^2 w_i(\lambda) \right)^2} \\ &\quad - \frac{(\sum_{i=1}^p (\xi_{\text{sp},i}^x)^2 w'_i(\lambda)) (\sum_{i=1}^p \xi_{\text{sp},i}^x \xi_{\text{sp},i}^z w_i(\lambda))}{\left( \sum_{i=1}^{n-p} (\xi_{\text{ns},i}^x)^2 + \sum_{i=1}^p (\xi_{\text{sp},i}^x)^2 w_i(\lambda) \right)^2}. \end{aligned}$$

So the denominator of  $f'(\lambda)$  is positive and the numerator is given by

$$\sum_{i,k} \xi_{\text{sp},i}^x \xi_{\text{sp},i}^z w'_i(\lambda) (\xi_{\text{ns},k}^x)^2 + \sum_{i,j} \xi_{\text{sp},i}^x \xi_{\text{sp},i}^z (\xi_{\text{sp},j}^x)^2 (w'_i(\lambda) w_j(\lambda) - w'_j(\lambda) w_i(\lambda)).$$

To consider the behaviour of the size of the bias, for simplicity assume that all  $\xi_{\text{sp},i}^x \xi_{\text{sp},i}^z$  are positive. Then the first term in the numerator of  $f'(\lambda)$  is positive. Note that this term is non-zero if and only if  $\mathbf{x}$  has non-spatial information. For the second term, we see that

$$\begin{aligned} w'_i(\lambda) w_j(\lambda) - w'_j(\lambda) w_i(\lambda) &= \frac{\alpha_i \sigma^{-2}}{(\sigma^{-2} + \lambda \alpha_i)^2} \frac{\lambda \alpha_j}{\sigma^{-2} + \lambda \alpha_j} + \frac{\alpha_j \sigma^{-2}}{(\sigma^{-2} + \lambda \alpha_j)^2} \frac{\lambda \alpha_i}{\sigma^{-2} + \lambda \alpha_i} \\ &= \frac{\lambda \alpha_i \alpha_j \sigma^{-2}}{(\sigma^{-2} + \lambda \alpha_i)(\sigma^{-2} + \lambda \alpha_j)} \left( \frac{1}{\sigma^{-2} + \lambda \alpha_i} - \frac{1}{\sigma^{-2} + \lambda \alpha_j} \right) \\ &= \frac{\lambda^2 \alpha_i \alpha_j \sigma^{-2}}{(\sigma^{-2} + \lambda \alpha_i)^2 (\sigma^{-2} + \lambda \alpha_j)^2} (\alpha_j - \alpha_i). \end{aligned}$$

So the second term of the numerator can be written as

$$\begin{aligned} &\sum_{i,j} \xi_{\text{sp},i}^x \xi_{\text{sp},i}^z (\xi_{\text{sp},j}^x)^2 c_{ij}(\lambda) (\alpha_j - \alpha_i) \\ &= \sum_{i < j} (\xi_{\text{sp},i}^x \xi_{\text{sp},i}^z (\xi_{\text{sp},j}^x)^2 - \xi_{\text{sp},j}^x \xi_{\text{sp},j}^z (\xi_{\text{sp},i}^x)^2) c_{ij}(\lambda) (\alpha_j - \alpha_i) \end{aligned}$$

where  $c_{ij}(\lambda) = c_{ji}(\lambda) = \frac{\lambda^2 \alpha_i \alpha_j \sigma^{-2}}{(\sigma^{-2} + \lambda \alpha_i)^2 (\sigma^{-2} + \lambda \alpha_j)^2} \geq 0$ . Since  $\alpha_j - \alpha_i \geq 0$  for  $i < j$  this shows that confounding at low frequencies ( $\xi_{\text{sp},i}^x \xi_{\text{sp},i}^z \neq 0$ ) contribute positively to the second term of  $f'(\lambda)$  whereas confounding at high frequencies ( $\xi_{\text{sp},j}^x \xi_{\text{sp},j}^z \neq 0$ ) contribute negatively. Conversely, unconfounded high frequencies ( $\xi_{\text{sp},j}^x \neq 0, \xi_{\text{sp},j}^z = 0$ ) contribute positively, while unconfounded low frequencies ( $\xi_{\text{sp},i}^x \neq 0, \xi_{\text{sp},i}^z = 0$ ) contribute negatively.

Our analysis therefore shows that the function  $f(\lambda)$ , i.e. the size of the bias in the spatial model as a function of  $\lambda$ , is quite complicated and the overall shape of the function depends on the confounding scenario. However, if there is a relatively large proportion of non-spatial information or unconfounded high frequency spatial

components in  $\mathbf{x}$ , then we can expect the behaviour of the first term in the derivative to dominate so that  $f(\lambda)$  is (at least broadly) an increasing function, i.e. it is in line with the intuition that more smoothing leads to larger bias.

*Proof of Corollary 3.* From the limiting behaviour of the weights  $w_i(\lambda)$ , it follows directly that

$$\lim_{\lambda \rightarrow \infty} f(\lambda) = \frac{\sum_{\{i|\alpha_i \neq 0\}} \xi_{\text{sp},i}^x \xi_{\text{sp},i}^z}{\sum_{i=1}^{n-p} (\xi_{\text{ns},i}^x)^2 + \sum_{\{i|\alpha_i \neq 0\}} (\xi_{\text{sp},i}^x)^2}.$$

For the limit as  $\lambda \rightarrow 0$ , we see that  $f(\lambda) = \frac{\text{Num}(\lambda)}{\text{Den}(\lambda)}$  where

$$\text{Num}'(\lambda) = \sum_{i=1}^p \xi_{\text{sp},i}^x \xi_{\text{sp},i}^z w_i'(\lambda), \quad \text{Den}'(\lambda) = \sum_{i=1}^p (\xi_{\text{sp},i}^x)^2 w_i'(\lambda).$$

Therefore, using l'Hôpital's rule,

$$\lim_{\lambda \rightarrow 0} f(\lambda) = \begin{cases} 0 & \text{if } \xi_{\text{ns}}^x \neq \mathbf{0} \\ \lim_{\lambda \rightarrow 0} \frac{\text{Num}'(\lambda)}{\text{Den}'(\lambda)} = \frac{\sum_{i=1}^p \xi_{\text{sp},i}^x \xi_{\text{sp},i}^z \alpha_i}{\sum_{i=1}^p (\xi_{\text{sp},i}^x)^2 \alpha_i} & \text{otherwise} \end{cases}.$$

□

Note that in the case where  $\mathbf{x}$  has no non-spatial components, the bias doesn't go to 0 as  $\lambda \rightarrow 0$ , however, the limit can still become close to 0 if  $\mathbf{x}$  has large unconfounded high frequency components. This is in line with the intuition that unconfounded high frequency components affect the bias in a similar way to non-spatial components.

## 1.7 Variance inflation

The literature on spatial confounding generally focuses on the bias in covariate effect estimates, but some papers (Reich et al., 2006; Zimmerman and Ver Hoef, 2022) also mention ‘‘variance inflation’’ in the spatial model compared to the non-spatial model. This can be explained by the following results.

Firstly, we compute expressions for the variance of the covariate effect estimates in the spatial model (3) and the non-spatial model (4). We see that, as was the case for the bias, the expressions agree except that the spatial model uses the metric defined by  $\Sigma^{-1}$  whereas in the non-spatial model, this is replaced by the usual Euclidean metric.

**Proposition A.1.** *Let  $\mathbf{U}$  be the orthonormal eigenbasis which diagonalises  $\Sigma^{-1}$ , and  $\xi^x = (\xi_{\text{ns}}^{xT}, \xi_{\text{sp}}^{xT})^T$  the coordinates of  $\mathbf{x}$  in this basis. The variance of the estimated covariate effect  $\hat{\beta}$  in model (3) is given by*

$$\text{Var}(\hat{\beta}) = \sigma^2 \frac{\langle \mathbf{x}, \mathbf{x} \rangle_{(\Sigma^{-1})^2}}{\langle \mathbf{x}, \mathbf{x} \rangle_{\Sigma^{-1}}} = \sigma^2 \frac{\sum_{i=1}^{n-p} (\xi_{\text{ns},i}^x)^2 + \sum_{i=1}^p (\xi_{\text{sp},i}^x)^2 w_i^2}{\left( \sum_{i=1}^{n-p} (\xi_{\text{ns},i}^x)^2 + \sum_{i=1}^p (\xi_{\text{sp},i}^x)^2 w_i \right)^2},$$

where  $w_i = \lambda \alpha_i / (\sigma^{-2} + \lambda \alpha_i)$  for  $i = 1, \dots, p$ .

*Proof.* Since under the data generating model (2)  $\text{Var}(\mathbf{y}) = \sigma^2 \mathbf{I}$ , we have that

$$\begin{aligned}\text{Var}(\widehat{\beta}) &= (\mathbf{x}^T \Sigma^{-1} \mathbf{x})^{-2} (\mathbf{x}^T \Sigma^{-1}) \text{Var}(\mathbf{y}) (\mathbf{x}^T \Sigma^{-1})^T \\ &= \sigma^2 (\mathbf{x}^T \Sigma^{-1} \mathbf{x})^{-2} \mathbf{x}^T (\Sigma^{-1})^2 \mathbf{x} \\ &= \sigma^2 \frac{\langle \mathbf{x}, \mathbf{x} \rangle_{(\Sigma^{-1})^2}}{\langle \mathbf{x}, \mathbf{x} \rangle_{\Sigma^{-1}}}.\end{aligned}$$

As  $(\Sigma^{-1})^2$  has eigenvalues  $\{\sigma^{-4}, \sigma^{-4}w_1^2, \dots, \sigma^{-4}w_p^2\}$  and is also diagonalised in the eigenbasis  $\mathbf{U}$ , the result follows (as in the proof of Corollary 1) by writing the above expression in the coordinates  $\xi^x$ .  $\square$

The proof of the following corollary is given in Appendix 1.8 below.

**Corollary A.1.** *Let  $\mathbf{U}$  be the orthonormal eigenbasis which diagonalises  $\Sigma^{-1}$ , and  $\xi^x = (\xi_{\text{ns}}^{xT}, \xi_{\text{sp}}^{xT})^T$  the coordinates of  $\mathbf{x}$  in this basis. The variance of the estimated covariate effect  $\widehat{\beta}_{\text{ns}}$  in model (4) is given by*

$$\text{Var}(\widehat{\beta}_{\text{ns}}) = \sigma^2 \langle \mathbf{x}, \mathbf{x} \rangle^{-1} = \frac{\sigma^2}{\sum_{i=1}^{n-p} (\xi_{\text{ns},i}^x)^2 + \sum_{i=1}^p (\xi_{\text{sp},i}^x)^2}.$$

Combining Proposition A.1 and Corollary A.1 we get the following results about the variance of the effect estimate in the spatial model.

**Corollary A.2.** *Let  $\mathbf{U}$  be the orthonormal eigenbasis which diagonalises  $\Sigma^{-1}$ , and  $\xi^x = (\xi_{\text{ns}}^{xT}, \xi_{\text{sp}}^{xT})^T$  the coordinates of  $\mathbf{x}$  in this basis. The expressions for the variances  $\text{Var}(\widehat{\beta})$  and  $\text{Var}(\widehat{\beta}_{\text{ns}})$  in the spatial and non-spatial model, respectively, satisfy the inequality  $\text{Var}(\widehat{\beta}) \geq \text{Var}(\widehat{\beta}_{\text{ns}})$ . We also have the following limiting behaviour of  $\text{Var}(\widehat{\beta})$ :*

$$\begin{aligned}\lim_{\lambda \rightarrow 0} \text{Var}(\widehat{\beta}) &= \frac{\sigma^2}{\sum_{i=1}^{n-p} (\xi_{\text{ns},i}^x)^2}, \\ \lim_{\lambda \rightarrow \infty} \text{Var}(\widehat{\beta}) &= \frac{\sigma^2}{\sum_{i=1}^{n-p} (\xi_{\text{ns},i}^x)^2 + \sum_{\{i \mid \alpha_i \neq 0\}} (\xi_{\text{sp},i}^x)^2},\end{aligned}$$

where the limit  $\lambda \rightarrow 0$  assumes that  $\xi_{\text{ns}}^{xT} \neq \mathbf{0}$ .

*Proof.* Recall from Appendix 1.6 that each weight  $w_i$  has  $0 \leq w_i < 1$  and increases as a function of the overall smoothing parameter  $\lambda$  with  $\lim_{\lambda \rightarrow 0} w_i(\lambda) = 0$  and  $\lim_{\lambda \rightarrow \infty} w_i(\lambda) = 1$ . Also, let

$$\begin{aligned}C_{\text{ns}} &= \sum_{i=1}^{n-p} (\xi_{\text{ns},i}^x)^2 \geq 0, \\ c_{\text{sp},i} &= (\xi_{\text{sp},i}^x)^2 \geq 0 \quad \text{for } i = 1, \dots, p.\end{aligned}$$

Then Proposition A.1 and Corollary A.1 show that

$$\begin{aligned}\text{Var}(\hat{\beta}) &= \sigma^2 \frac{C_{\text{ns}} + \sum_{i=1}^p c_{\text{sp},i} w_i^2}{(C_{\text{ns}} + \sum_{i=1}^p c_{\text{sp},i} w_i)^2}, \\ \text{Var}(\hat{\beta}_{\text{ns}}) &= \frac{\sigma^2}{C_{\text{ns}} + \sum_{i=1}^p c_{\text{sp},i}} \\ &= \sigma^2 \frac{C_{\text{ns}} + \sum_{i=1}^p c_{\text{sp},i} w_i^2}{(C_{\text{ns}} + \sum_{i=1}^p c_{\text{sp},i})(C_{\text{ns}} + \sum_{i=1}^p c_{\text{sp},i} w_i^2)}\end{aligned}$$

So the difference between the two expressions is the denominators:

$$\begin{aligned}\text{Den}_{\text{sp}} &= \left( C_{\text{ns}} + \sum_{i=1}^p c_{\text{sp},i} w_i \right)^2, \\ \text{Den}_{\text{ns}} &= \left( C_{\text{ns}} + \sum_{i=1}^p c_{\text{sp},i} \right) \left( C_{\text{ns}} + \sum_{i=1}^p c_{\text{sp},i} w_i^2 \right).\end{aligned}$$

Thus, to show that  $\text{Var}(\hat{\beta}_{\text{ns}}) \leq \text{Var}(\hat{\beta})$ , it suffices to show that  $\text{Den}_{\text{sp}} \leq \text{Den}_{\text{ns}}$ . We have that

$$\begin{aligned}\text{Den}_{\text{ns}} - \text{Den}_{\text{sp}} &= C_{\text{ns}}^2 + \sum_{i,j=1}^p c_{\text{sp},i} c_{\text{sp},j} w_j^2 + C_{\text{ns}} \sum_{i=1}^p c_{\text{sp},i} (w_i^2 + 1) \\ &\quad - C_{\text{ns}}^2 - \sum_{i,j=1}^p c_{\text{sp},i} w_i c_{\text{sp},j} w_j - 2C_{\text{ns}} \sum_{i=1}^p c_{\text{sp},i} w_i \\ &= \sum_{i,j=1}^p c_{\text{sp},i} c_{\text{sp},j} (w_j^2 - w_i w_j) + C_{\text{ns}} \sum_{i=1}^p c_{\text{sp},i} (w_i - 1)^2 \\ &\geq \sum_{i,j=1}^p c_{\text{sp},i} c_{\text{sp},j} (w_j^2 - w_i w_j) \\ &= \sum_{i < j}^p c_{\text{sp},i} c_{\text{sp},j} (w_j^2 - w_i w_j + w_i^2 - w_j w_i) \\ &= \sum_{i < j}^p c_{\text{sp},i} c_{\text{sp},j} (w_j - w_i)^2 \geq 0.\end{aligned}$$

Hence  $\text{Var}(\hat{\beta}_{\text{ns}}) \leq \text{Var}(\hat{\beta})$ .

The limits  $\lim_{\lambda \rightarrow 0} \text{Var}(\hat{\beta})$  and  $\lim_{\lambda \rightarrow \infty} \text{Var}(\hat{\beta})$  follow directly from inserting the limits  $\lim_{\lambda \rightarrow 0} w_i(\lambda) = 0$  and  $\lim_{\lambda \rightarrow \infty} w_i(\lambda)$  into the expression for  $\text{Var}(\hat{\beta})$ .  $\square$

Corollary A.2 appears to prove that the variance in the spatial model is indeed inflated compared to that of the non-spatial model. However, an important note here is that the parameter  $\sigma^2$  is usually estimated, and the estimate in the non-spatial model is likely to be somewhat bigger than the estimate in the spatial model (because the spatial

effects approximate the unmeasured spatial variation  $\mathbf{z}$  whereas the non-spatial model treats  $\mathbf{z}$  as largely unexplained.) Therefore, the estimated variance in the non-spatial model will typically be larger than in the spatial model, and this is in fact what is often seen in practice.

Note that for the same value of  $\sigma^2$ , the effect of the ‘‘variance inflation’’ tends to be small when either  $\lambda$  is large or the proportion of spatial information in  $\mathbf{x}$  is small. This is in line with intuition as smoothing is expected to decrease the variance of the spatial model estimates (and large values of  $\lambda$  give more smoothing), and less spatial information in  $\mathbf{x}$  should lead to less uncertainty around what relates to the covariate as opposed to the spatial effects.

## 1.8 Proof of Corollaries 2 and A.1

*Proof.* The model (4) can be viewed as a spatial model (3) with a single unsmoothed spatial basis vector spanning the intercept, that is,  $\mathbf{B}_{\text{sp}} = [b_1]$  where  $b_1 = (1, \dots, 1)^T$  and  $w_1 = \alpha_1 = 0$ . Inserting this into the expression for  $\Sigma^{-1}$  and using the fact that  $b_1^T b_1 = n$  then gives that

$$\Sigma^{-1} = \sigma^{-2}(\mathbf{I} - \frac{1}{n}b_1 b_1^T), \quad (\Sigma^{-1})^2 = \sigma^{-2}\Sigma^{-1}.$$

Under the assumption that  $\mathbf{x}$  is centered we have that  $\mathbf{x}^T b_1 = 0$  and, therefore,

$$\langle \mathbf{x}, \mathbf{z} \rangle_{\Sigma^{-1}} = \sigma^{-2} \mathbf{x}^T (\mathbf{I} - \frac{1}{n}b_1 b_1^T) \mathbf{z} = \sigma^{-2} \langle \mathbf{x}, \mathbf{z} \rangle.$$

Similarly,

$$\langle \mathbf{x}, \mathbf{x} \rangle_{\Sigma^{-1}} = \sigma^{-2} \langle \mathbf{x}, \mathbf{x} \rangle \quad \text{and} \quad \langle \mathbf{x}, \mathbf{x} \rangle_{(\Sigma^{-1})^2} = \sigma^{-4} \langle \mathbf{x}, \mathbf{x} \rangle.$$

The results then follow from Propositions 1 and A.1.  $\square$

## 2 Reparameterisation of spatial effects

In Scenario 3 of the simulation study and when implementing the capped spatial+, we use reparameterisation of the TPRS spatial effect. In this section, we explain how this reparametrisation is obtained. Recall Equation (3) and  $\beta_{\text{sp}} \sim N(\mathbf{0}, \lambda^{-1}\mathbf{S}^-)$ . We can use an eigendecomposition to diagonalise  $\mathbf{S} = \mathbf{U}\Lambda\mathbf{U}^T$  where  $\Lambda$  is a diagonal matrix of the eigenvalues  $\alpha_1, \dots, \alpha_p$  and  $\mathbf{U}$  contains the associated eigenvectors. In order to consider, for example, only the  $k$  highest frequencies from the spatial effect, we reparameterise the model such that  $\tilde{\mathbf{B}}_{\text{sp}} = \mathbf{B}_{\text{sp}} \tilde{\mathbf{U}}$  and  $\tilde{\beta}_{\text{sp}} \sim N(\mathbf{0}, \lambda^{-1}(\tilde{\Lambda})^-)$ , where  $\tilde{\mathbf{U}}$  and  $\tilde{\Lambda}$  are  $p \times (p - k)$  and  $(p - k) \times (p - k)$  matrices, respectively, associated with  $\mathbf{U}$  and  $\Lambda$  after removing the columns associated with the  $k$  highest frequencies. In Scenario 3 of the simulation study, this reparametrisation is used to generate  $\mathbf{z}_{\text{sp},h}$  and  $\mathbf{z}_{\text{sp},l}$  and in Section 5.4, this reparameterised spatial effect without the  $k$  highest frequencies is used in the capped spatial+ in both the first and second order equations.

In Section 5.4, the same method is used to generate  $\mathbf{z}_{\text{sp},\text{low}}^x$ ,  $\mathbf{z}_{\text{sp},\text{medium}}^x$ , or  $\mathbf{z}_{\text{sp},\text{high}}^x$ , where we choose the relevant frequencies and reparameterise the spatial effect as described above.

### 3 Additional simulation results

#### 3.1 MSE of fitted values

Figure 7 shows the MSE of fitted values for the several models in Scenarios 1–4 of the simulation study as well as the simulations for capped spatial+. For Scenarios 1–4, as expected, the non-spatial model generally has a worse fit than the spatial model as it is mis-specified.

#### 3.2 Scenario 3: Comparison to the non-spatial model

Here, we repeat Scenario 1 but with a larger proportion of unconfounded low frequency components in  $\mathbf{x}$  so that the correlation between  $\mathbf{x}$  and  $\mathbf{z}$  is low overall, but high at high frequencies. Specifically, we consider  $\xi_{\text{sp},h}^x = 1$ ,  $\xi_{\text{sp},1}^z = 0$ ,  $\xi_{\text{sp},1}^x \in \{1, 20\}$  and  $\xi_{\text{sp},h}^z \in \{0.2, 0.5, 1\}$  (with  $\xi_{\text{sp},1}^x = 1$  corresponding to Scenario 1). For both models, the coefficient  $\xi_{\text{sp},1}^x$  only contributes to the denominator of the bias. In the spatial model, this contribution is multiplied by relatively small weights  $w_i$ , whereas in the non-spatial model all weights are 1. Therefore, increasing  $\xi_{\text{sp},1}^x$  keeping everything else fixed should reduce the bias in both models, but with a much larger effect on the non-spatial bias. The results in Figure 6 (left) confirm this, and we see that bias in the spatial model now exceeds the non-spatial bias.

### 4 Simulation results using Gaussian Processes in the DGP

In this section we extend the simulation results of Section 4. As an alternative to using the thin plate regression splines to generate low and high frequency spatial fields  $\mathbf{z}_{\text{sp},1}$  and  $\mathbf{z}_{\text{sp},h}$ , here we use Gaussian processes. The analysing spatial model still uses thin plate regression splines, thus we are in a mis-specified model setting. Compared to Section 4, mis-specification bias may occur in addition to the confounding bias. However, generally, conclusions in each scenario follow quite closely to those in Section 4.

In order to generate the data, we start by considering a mean-zero Gaussian process  $\gamma$  with exponential covariance structure following  $C(h) = \exp(-h/\kappa)$  such data  $h = \|\mathbf{s} - \mathbf{s}'\|$  for  $\mathbf{s}, \mathbf{s}' \in [0, 1] \times [0, 1]$ , which is assumed for the sake of simplicity to have variance of 1. We set  $\kappa = 0.3$  corresponding to a spatial range of approximately 0.3. Let  $\Sigma_{\text{sp}}$  be the positive-definite spatial covariance matrix of  $\gamma$  and consider its eigendecomposition  $\Sigma_{\text{sp}} = \mathbf{V}_{\text{sp}} \Lambda \mathbf{V}_{\text{sp}}^T$  where  $\mathbf{V}_{\text{sp}}$  is an orthogonal matrix of eigenvectors of  $\Sigma_{\text{sp}}$  and  $\Lambda$  is a diagonal matrix that contains the corresponding eigenvalues in descending order. We take the first 10 largest eigenvalues of  $\Sigma_{\text{sp}}$  and define the  $\Sigma_{\text{sp},l} = \mathbf{V}_{\text{sp},l} \Lambda_l \mathbf{V}_{\text{sp},l}^T$  where  $\mathbf{V}_{\text{sp},l}$  and  $\Lambda_l$  are the submatrices of  $\mathbf{V}_{\text{sp}}$  and  $\Lambda$ , respectively, associated with the 10 largest eigenvalues. Let the square root of  $\Sigma_{\text{sp},l}$  be  $\mathbf{L}_{\text{sp},l}^{1/2} = \mathbf{V}_{\text{sp},l} \Lambda_l^{1/2} \mathbf{V}_{\text{sp},l}^T$ . Then,  $\mathbf{z}_{\text{sp},l} = \mathbf{L}_{\text{sp},l} \zeta_l$  where  $\zeta_l$  follows a standard normal distribution. We take the remaining  $n - 10$  eigenvalues of  $\Sigma_{\text{sp}}$  and define  $\mathbf{L}_{\text{sp},h} = \mathbf{V}_{\text{sp},h} \Lambda_h^{1/2} \mathbf{V}_{\text{sp},h}^T$  such that  $\mathbf{z}_{\text{sp},h} = \mathbf{L}_{\text{sp},h} \zeta_h$  where  $\zeta_h$  follows a standard

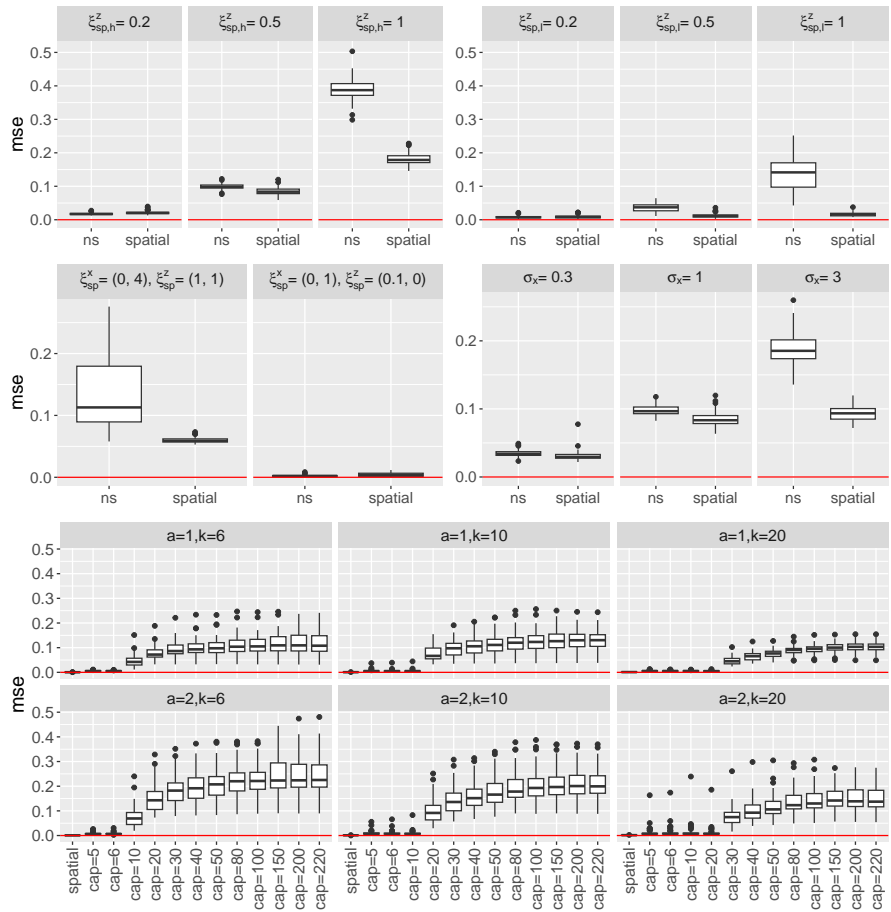


Figure 5: MSE of fitted values in the spatial and non-spatial (ns) models under Scenario 1 (top, left), Scenario 2 (top, right), Scenario 3 (middle, left), Scenario 4 (middle, right). MSE of fitted values in simulations for capped spatial+ (bottom).

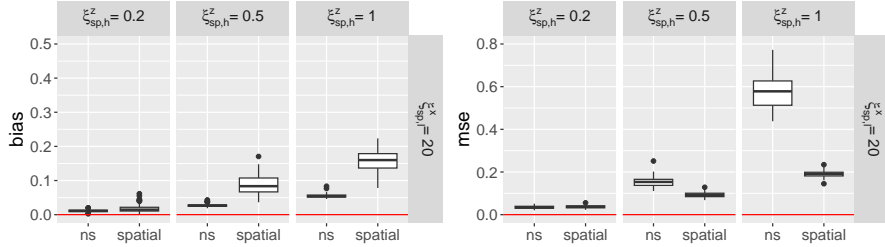


Figure 6: Bias of  $\hat{\beta}$  and  $\hat{\beta}_{ns}$  (left) and mean squared error of fitted values (right) in the spatial and non-spatial (ns) models under the additional simulations for Scenario 3. The true value of  $\beta$  is 0.5.

normal distribution. Note that the spatial covariance matrix of the Gaussian process has full rank  $n$  and we use all eigenvalues to generate  $\mathbf{z}_{sp,l}$  and  $\mathbf{z}_{sp,h}$ , so the spatial basis vectors span the whole space, i.e the noise term in  $\mathbf{x}$  is unconfounded in the sense that it is generated independently from the spatial effect  $\mathbf{z}$ , but it still is a linear combination of the spatial basis vectors. The spatial analysis model uses thin plate regression splines with 300 basis functions.

Some details are skipped in the following sections as they overlap both in terms of expectations and final conclusions to those in Section 4. For a more detailed reflection on the results, we recommend consulting Section 4.

#### 4.1 Scenario 1: Confounding at high frequencies

We consider  $(\xi_{sp,l}^x, \xi_{sp,h}^x) = (1, 1)$ ,  $\xi_{sp,l}^z = 0$  and  $\xi_{sp,h}^z \in \{0.5, 2, 3\}$ . The results in Figure 7 follow similarly to Scenario 1 in 4. As expected, large contributions to bias in the spatial model happen when there is confounding at high frequencies, and the size of the bias increases linearly with  $\xi_{sp,h}^z$  (as everything else is held fixed). The same logic follows for the non-spatial model and, for this particular data generating process, the bias of the non-spatial model is always larger than the one in the spatial model.

#### 4.2 Scenario 2: Confounding at low frequencies

As before, we swap high and low frequencies in  $\mathbf{z}$ , such that there is only confounding at low frequencies. We consider  $(\xi_{sp,l}^x, \xi_{sp,h}^x) = (1, 1)$ ,  $\xi_{sp,h}^z = 0$  and  $\xi_{sp,l}^z \in \{0.5, 2, 3\}$ . The results in Figure 7 follow similarly to Scenario 2 in Section 4. When confounding only happens at low frequencies, the bias is close to zero in the spatial model and remains close to zero as  $\xi_{sp,l}^z$  increases, even despite potential model misspecification. Thus, the thin plate regression splines generally seem able to capture the behavior of the Gaussian process used in the data generating process. In contrast, the non-spatial model has a positive and linearly increasing bias, similar to Scenario 2 in Section 4, since all terms are weighted by 1, as opposed to the spatial model where lower frequencies have lower weights.

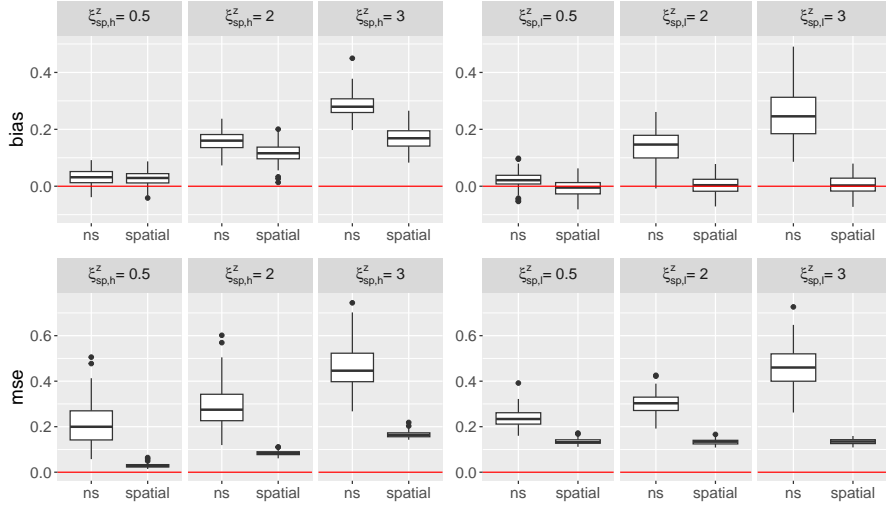


Figure 7: Bias of  $\hat{\beta}$  and  $\hat{\beta}_{ns}$  (top) and mean squared error of fitted values (bottom) in the spatial and non-spatial (ns) models under Scenarios 1 (left) and 2 (right). The true value of  $\beta$  is 0.5.

### 4.3 Scenario 3: Comparison to a non-spatial model

We consider  $\xi_{sp,h}^x = 1$ ,  $\xi_{sp,l}^x = 0$ ,  $\xi_{sp,l}^z \in \{5, 10\}$  and  $\xi_{sp,h}^z \in \{0.5, 2, 3\}$ . The results in Figure 8 follow similarly to Scenario 3 in Section 4; by increasing  $\xi_{sp,l}^z$  we can reach data generating processes where the non-spatial model has smaller bias than the spatial model, because the correlation between  $\mathbf{x}$  and  $\mathbf{z}$  is overall low (and thus non-spatial bias is low), but it is strong at high frequencies (inducing high spatial bias).

### 4.4 Scenario 4: Dependence on non-spatial information

We consider  $\sigma_x \in \{0.3, 1, 2, 3\}$ . Other parameters remain constant at  $(\xi_{sp,l}^x, \xi_{sp,h}^x) = (1, 1)$ ,  $(\xi_{sp,l}^z, \xi_{sp,h}^z) = (0, 2)$ . The results in Figure 9 follow similarly to Scenario 4 in Section 4 and the bias decreases for both the non-spatial and spatial model when  $\sigma_x$  is increased. Once again, the bias is larger in the non-spatial model than in the spatial, except when  $\sigma_x = 0.3$ .

### 4.5 Scenario 5: Dependence on the smoothing parameter

We consider  $(\xi_{sp,l}^x, \xi_{sp,h}^x) = (0, 1)$ ,  $(\xi_{sp,l}^z, \xi_{sp,h}^z) = (1, 1)$ ,  $\sigma_x = \sigma = 1$ , and fix  $\lambda$  to different values. We let  $\sigma_x \in \{0.3, 1, 2\}$ . The results are based on 20 replicates.

As can be observed in Figure 10, the higher the  $\sigma_x$  the lower the bias. For  $\sigma_x = 0.3$ , the spatial bias is mostly above the non-spatial bias and slowly converges to the non-spatial bias. Eventually, for  $\sigma_x = 2$ , the spatial bias is always below the non-spatial bias, until it reaches it for large  $\lambda$ . Compared to Scenario 5 in Section 4, a bias close

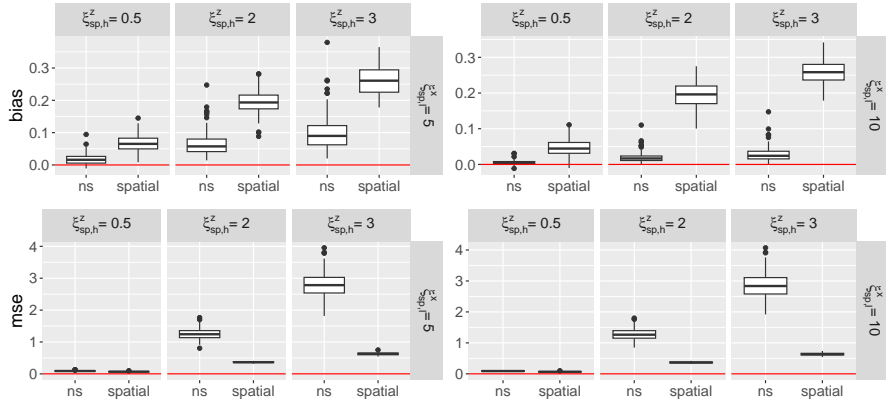


Figure 8: Bias of  $\hat{\beta}$  and  $\hat{\beta}_{ns}$  (top) and mean squared error of fitted values (bottom) in the spatial and non-spatial (ns) models under Scenario 3. The true value of  $\beta$  is 0.5.

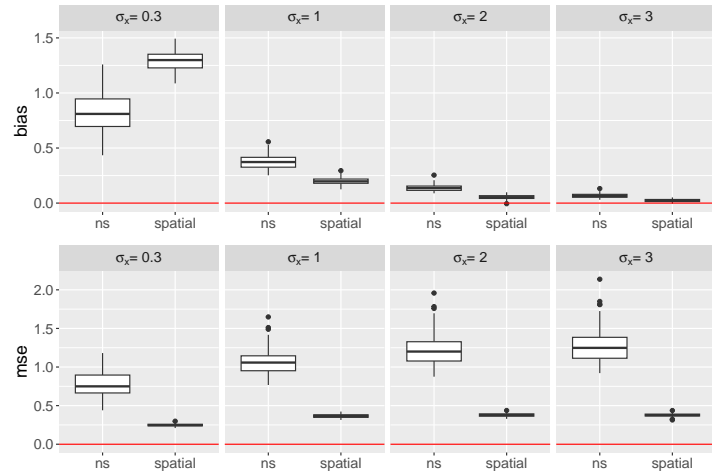


Figure 9: Bias of  $\hat{\beta}$  and  $\hat{\beta}_{ns}$  (top) and mean squared error of fitted values (bottom) in the spatial and non-spatial (ns) models under Scenario 4. The true value of  $\beta$  is 0.5.

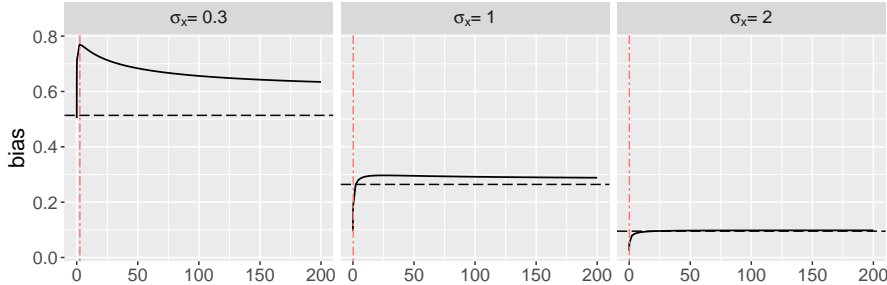


Figure 10: Bias of  $\hat{\beta}$  (solid black) and  $\hat{\beta}_{ns}$  (dashed black) for increasing  $\lambda$  and different  $\sigma_x$ . The true value of  $\beta$  is 0.5. The magenta dashed line shows the median  $\hat{\lambda}$  estimated by generalized cross-validation. The bias associated with each  $\hat{\lambda}$  is 0.7232, 0.1872, 0.0340, from left to right.

to 0 is never reached for  $\sigma_x = 0.3$ , most likely due to the presence of additional misspecification bias when using a Gaussian process as the data generating process. The generalized cross-validation estimate  $\hat{\lambda}$  always stays on the steep part of the spatial bias curve, indicating that small changes in  $\hat{\lambda}$  can lead to large changes in the spatial bias. The  $\hat{\lambda}$  for the highest two  $\sigma_x$  leads to a spatial bias lower than the non-spatial bias.

## References

Guan, Y., Page, G. L., Reich, B. J., Ventrucci, M., and Yang, S. (2023). Spectral adjustment for spatial confounding. *Biometrika*, 110(3):699—719.

Keller, J. P. and Szpiro, A. A. (2020). Selecting a scale for spatial confounding adjustment. *Journal of the Royal Statistical Society Series A: Statistics in Society*, 183(3):1121–1143.

Paciorek, C. J. (2010). The importance of scale for spatial-confounding bias and precision of spatial regression estimators. *Statistical Science*, 25(1):107–125.

Page, G. L., Liu, Y., He, Z., and Sun, D. (2017). Estimation and prediction in the presence of spatial confounding for spatial linear models. *Scandinavian Journal of Statistics*, 44(3):780–797.

Reich, B. J., Hodges, J. S., and Zadnik, V. (2006). Effects of residual smoothing on the posterior of the fixed effects in disease-mapping models. *Biometrics*, 62(4):1197–1206.

Zimmerman, D. L. and Ver Hoef, J. M. (2022). On deconfounding spatial confounding in linear models. *The American Statistician*, 76(2):159–167.